Supporting Information

Novel Covalent Organic Nanosheets for Construction of Ultrafine and Well-dispersed Metal Nanoparticles

Feipeng Lu, Yaqiong Li, Qingrong Shi, Chaofeng Zhao, Shenghua Li, * and Siping Pang*

School of Materials Science and Engineering, Beijing Institute of Technology, No.5 South Zhongguancun Street, Haidian District, Beijing 100081, P. R. China

Contents

1. General Information

Liquid 1H and 13C NMR spectra were collected with a Bruker Avance III 600MHz NMR spectrometer using tetramethylsilane (TMS) as an internal standard.

FT-IR spectra were recorded with Perkin Elmer 480 FTIR spectrophotometer (KBr pellet).

Powder X-ray diffraction (PXRD) data were collected with Rigaku mini Flex600 diffractometer operated at 40 kV and 15 mA with Cu Kα radiation (step size of 0.02^{o} and step time of 0.24 s).

Solid-state NMR experiments were performed on Bruker AVWBIII600 MHz spectrometer. The 13C CP/MAS NMR spectra were recorded with 4 mm double-resonance MAS probe and with sample spinning rate of 12 kHz.

The nitrogen adsorption-desorption isotherms were performed at 77 K with a Micromeritics ASAP 2460 system. Surface areas were calculated using Langmuir and Brunauer-Emmett-Teller (BET) methods, respectively. The pore-size-distribution curves were calculated from nitrogen adsorption isotherms using non-local density functional theory (NLDFT).

Thermogravimetric Analysis (TGA) measurements were conducted using Netzsch STA 449F3 thermogravimetric analysis instrument over the temperature range of 25 to 500 °C (with a heating rate of 5 °C min^{-1}) under nitrogen atmosphere.

Field emission scanning electron microscopy (SEM) observations were performed on JEOL BCPCAS4800 microscope operated at an accelerating voltage of 5.0 kV.

High Resolution Transmission electron microscopy (TEM) images were obtained with E. A. Fischione 300-025 operated at 300 kV.

Inductively Coupled Plasma Mass Spectrometry (ICP-MS) measurements were conducted using Agilent 7700.

2. Materials

Super dry reagents were purchased from Sun Chemical Technology (Shanghai) Co. Ltd. Other common reagents purchased from Beijing Chemical Industry Group Co. LTD. 1,3,5-Tris(4-formylphenyl)-benzene (TFP), 1,3,5-triformylbenzene (TFB), and 4,7-diamine-1H-indazole (DAI) were purchased from Jilin Chinese Academy of Science - Yanshen Technology Co. Ltd.

3. Experimental

3.1 Synthesis of model compound of COF-DAI-TFP:

1, 3, 5- Triformylphloroglucinol (TFP) (63 mg, 0.3 mmol) and 7-amino-1H-indazole (146 mg, 1.1 mmol) were added to a round-bottom flask. N-Methyl pyrrolidone (NMP, 15 mL) and acetic acid (6 M, 1 mL) were poured into the reaction. The reaction was heated to 80 °C with stir. After 6 hours, the reaction was cooled down to room temperature, the precipitate was collected via filtration. Then, the precipitate was washed with NMP (3 mL*

3), dioxane (5 mL* 3) and ethanol (5 mL* 5). Yellow solid was obtained after the precipitate was dried under vacuum for 10 h (100 °C).

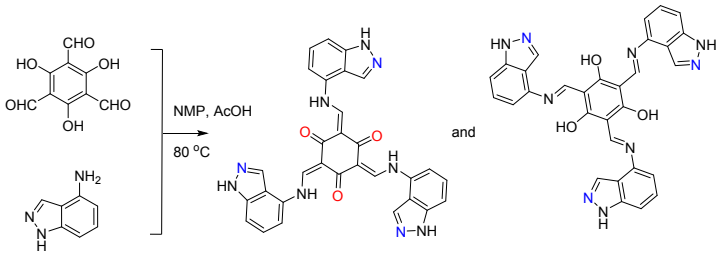

Scheme S1 the synthesis of model compound of COF-DAI-TFP

3.2 Synthesis of COF-DAI-TFP:

Pyrex tube (5 mL) was charged with TFP (17.4 mg, 0.08 mmol), 4,7-diamine-1H-indazole (DAI) (18.1 mg, 0.12 mmol), *o*-dichlorobenzene (1.3 mL) and methanol (0.7 mL). The resulting suspension was sonicated for 10 min at room temperature, and then acetic acid aqueous solution (0.2 mL, 6 M) was added to the tube. The tube was then freeze-pump-thaw 3 cycles and sealed off. The sealed tube was slowly heated to 100 °C and kept for 72 h. The resulted dark-red powder was collected by centrifuge, then washed with DMF (4 × 8 mL) and ethanol (4 × 8 mL). Finally, COF-DAI-TFP was obtained with 89% isolated yield after dried at 90 °C under vacuum for 24 hours.

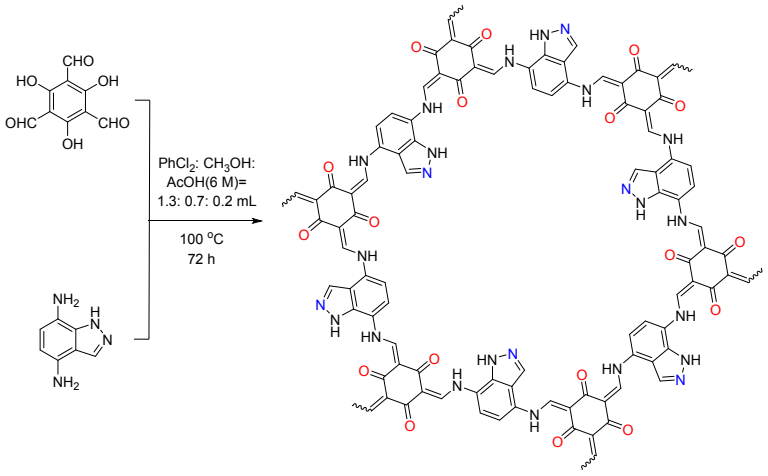

Scheme S2 the synthesis of COF-DAI-TFP

3.3 Synthesis of COF-DAI-TFB:

Pyrex tube (5 mL) was charged with TFB (13.2 mg, 0.08 mmol), 4,7-diamine-1H-indazole (DAI) (18.1 mg, 0.12 mmol), *o*-dichlorobenzene (1.3 mL) and methanol (0.7 mL). The resulting suspension was sonicated for 10 min at room temperature, and then acetic acid aqueous solution (0.2 mL, 3 M) was added to the tube. The tube was then freeze-pump-thaw 3 cycles and sealed off. The sealed tube was slowly heated to 100 °C and kept for 72 h. The resulted dark-red powder was collected by centrifuge, then washed with DMF (4 × 8 mL) and ethanol (4 × 8 mL). Finally, COF-DAI-TFB was obtained with 87% isolated yield after dried at 90 °C under vacuum for 24 hours.

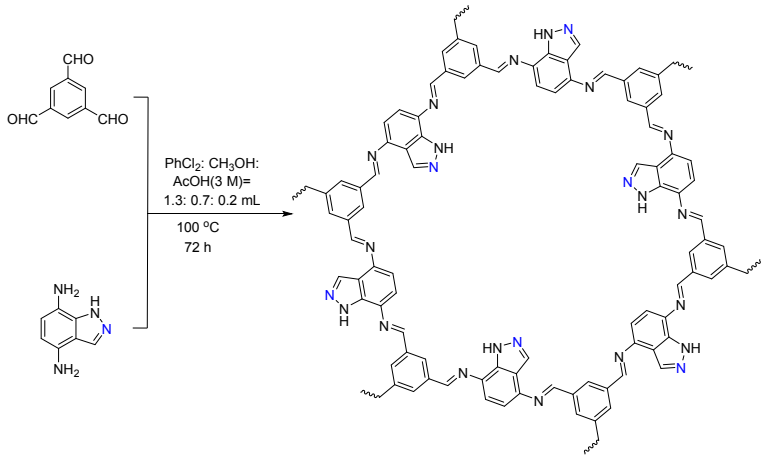

Scheme S3 the synthesis of COF-DAI-TFB

3.4 Synthesis of U-MNPs on COF-DAI-TFP (e. g. Pd, Ir, and Pt)

COFs (10 mg) were dispersed into ethanol (5 mL), metal precursors (K_2PdCl_6, $IrCl_3$, and K_2PtCl_6, 0.02 mmol) were dissolved in water (3 mL). The metal precursors were deposited onto COF-DAI-TFP, by mixing metal precursor aqueous solution with COF-DAI-TFP suspension in methanol and evaporating all the solvent under vacuum with stirring. The metal precursor on COF-DAI-TFP was re-dispersed in ethanol (10 mL) and stirred for 1 h. $NaBH_4$ (2 mmol) was added to the ethanol solution and stirred for 15 h. Centrifugation was used to obtain the metal NPs on COF-DAI-TFP, then these materials were washed with ethanol and water mixed solution (V: V 1: 1, 8* 10 mL), then washed with ethanol (5* 6 mL). Finally, U-MNPs on COF-DAI-TFP (M@COF-DAI-TFP) were dried under vacuum at room temperature for 12 h before the characterization and further use.

3.5 Reduction of *p*-aminophenol with the catalysis of M@COF-DAI-TFP

M@COF-DAI-TFP was dispersed into aqueous solution easily via slightly ultrasonic treatment, which shows feasibility as heterogeneous catalyst. The aqueous suspension of M@COF-DAI-TFP (0.5 mg mL^{-1}, 30 μL) was added to the mixture of water (1 mL), *p*-nitrophenol (1 mM, 0.3 mL), and $NaBH_4$ (0.5 M, 1 mL) aqueous solution.

Cyclic catalysis experiment with the catalysis of the dated Pd@COF-DAI-TFP was conducted with the following method. Keeping the amount of Pd@COF-DAI-TFP (0.5 mg mL-1, 30 μL), water (1 mL), and $NaBH_4$ (0.5 M, 1 mL). Additional *p*-nitrophenol (1 mM; 0.3 mL for 1st, 0.345 mL for 2st, 0.397 mL for 3st, 0.456 mL for 4st, 0.525 mL for 5st) was added to the cuvette upon the previous reduction completed. Meanwhile, the reduction process was monitored by UV-Vis spectroscopy.

4. NMR and FTIR Spectrum of raw materials

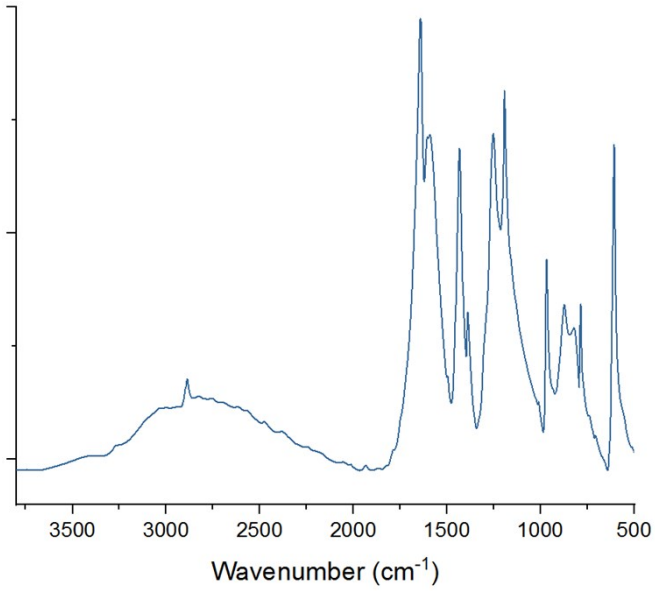

Figure S 1 The FT-IR spectra of TFP.

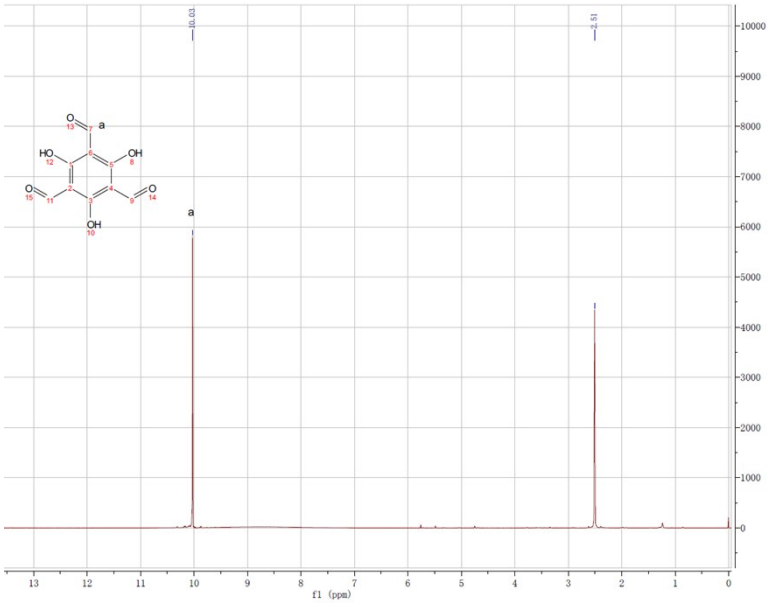

Figure S 2 The ^{1}H-NMR of TFP (DMSO-d6)

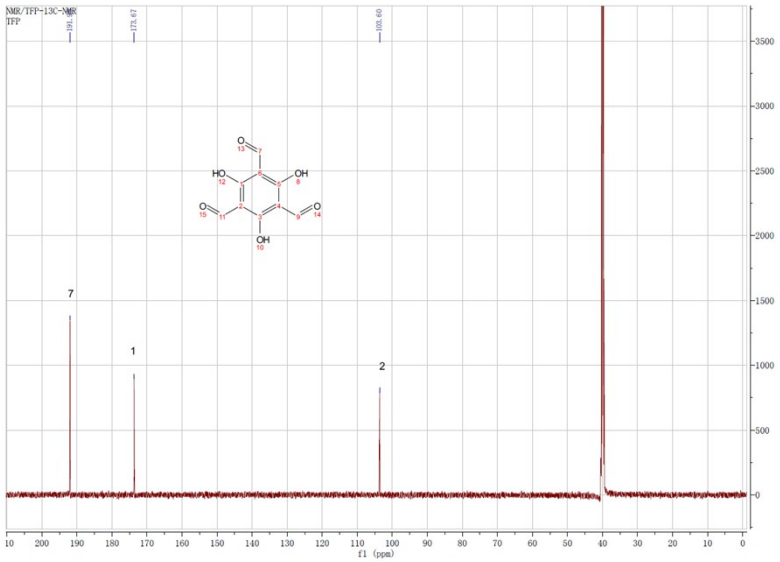

Figure S 3 The ^{13}C-NMR of TFP (DMSO-d6).

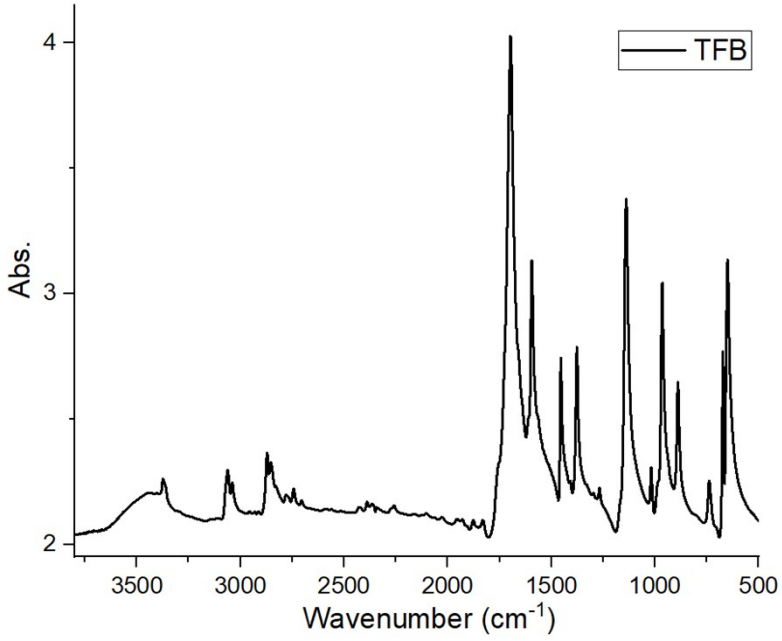

Figure S 4 The FT-IR spectra of TFB.

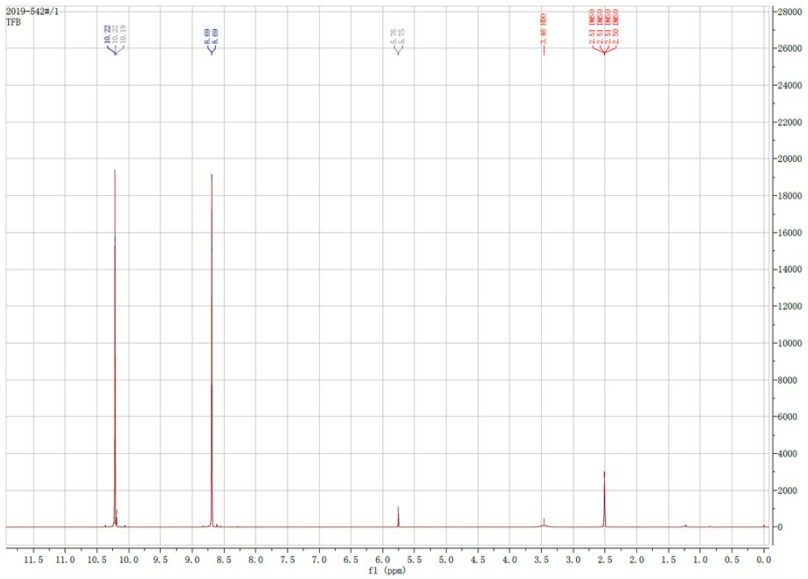

Figure S 5 The ^{1}H-NMR of TFB (DMSO-d6).

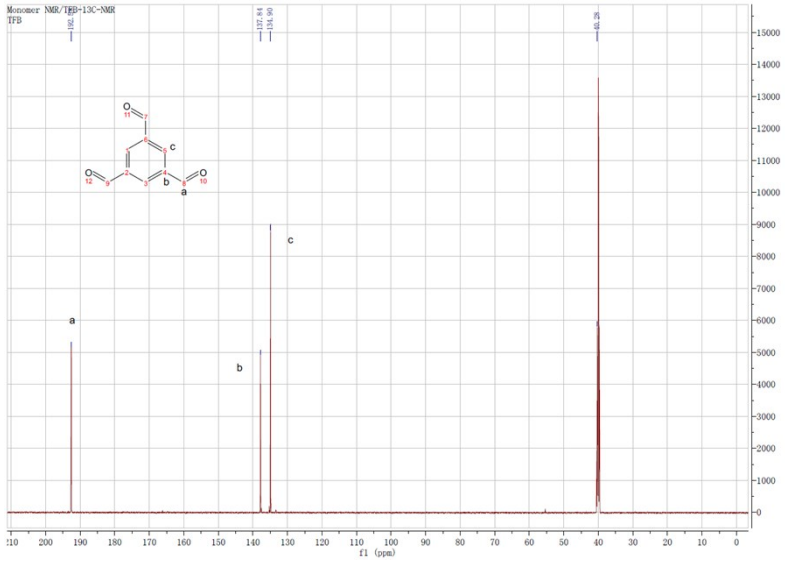

Figure S 6 The ^{13}C-NMR of TFB (DMSO-d6).

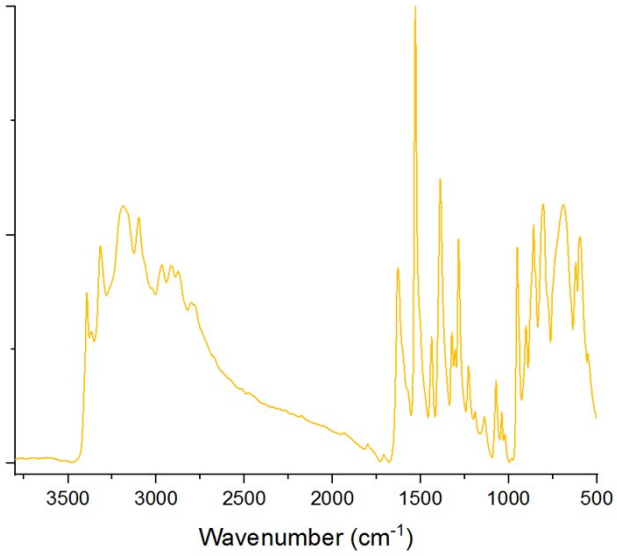

Figure S 7 The FT-IR spectra of DAI.

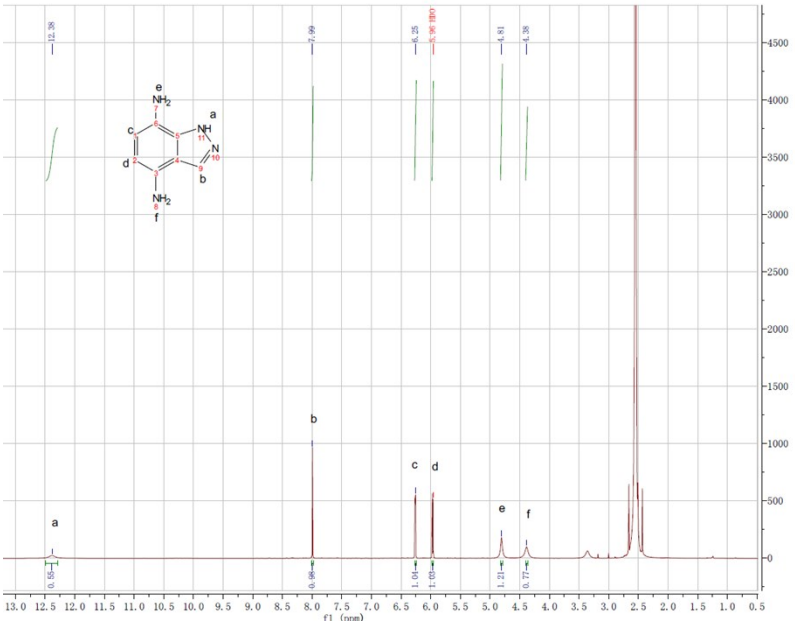

Figure S 8 The ^{1}H-NMR of DAI (DMSO-d6).

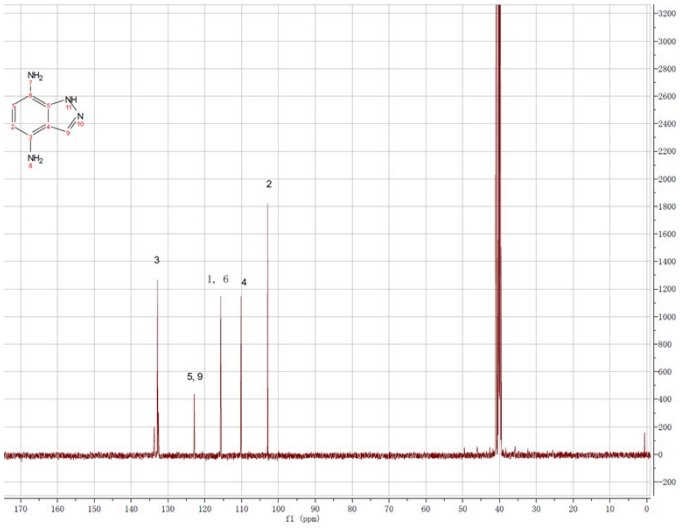

Figure S 9 The ^{13}C-NMR of DAI (DMSO-d6).

5. NMR and FTIR Spectrum of model compounds for COF-DAI-TFP and COF-DAI-TFB

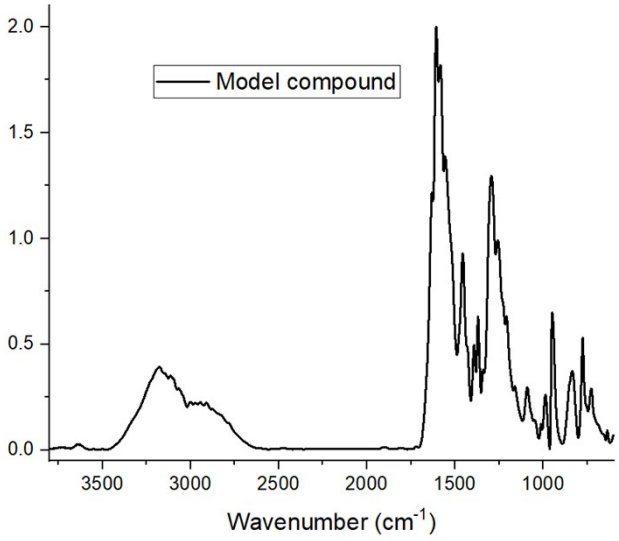

Figure S 10 The FT-IR spectra of the model compound for COF-DAI-TFP.

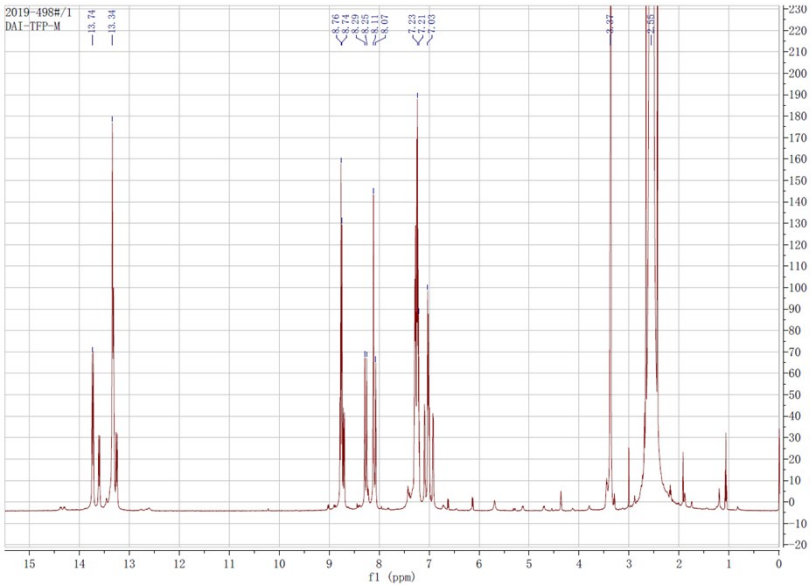

Figure S 11 The ^{1}H-NMR of the model compound for COF-DAI-TFP (DMSO-d6).

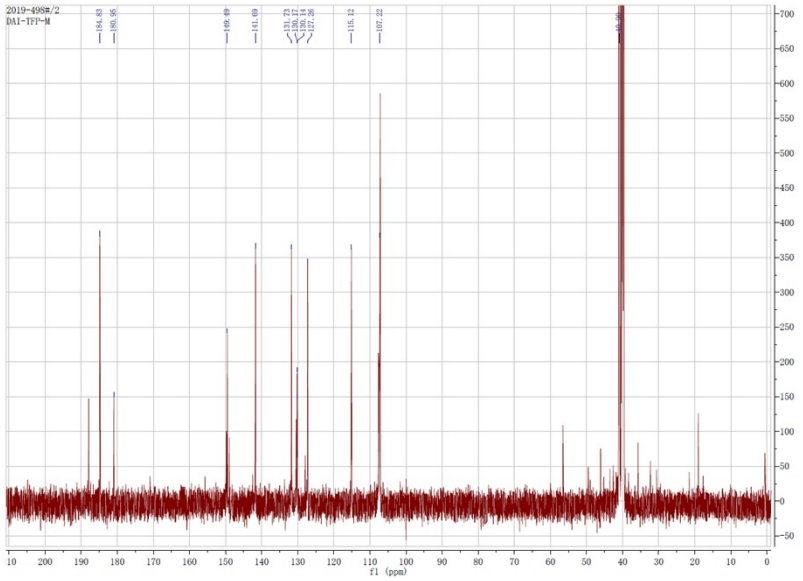

Figure S 12 The ^{13}C-NMR of the model compound for COF-DAI-TFP (DMSO-d6).

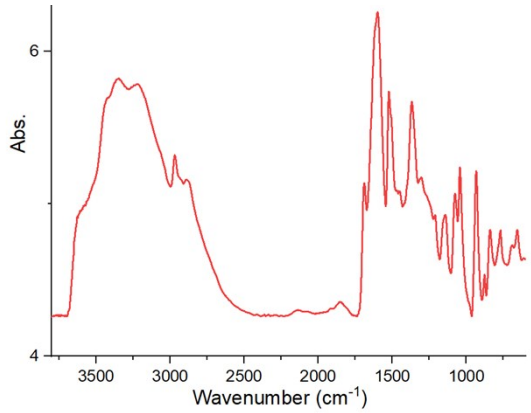

Figure S 13 The FT-IR spectra of the model compound for COF-DAI-TFB.

6. Optimized structure for COF-DAI-TFB (DFT method)

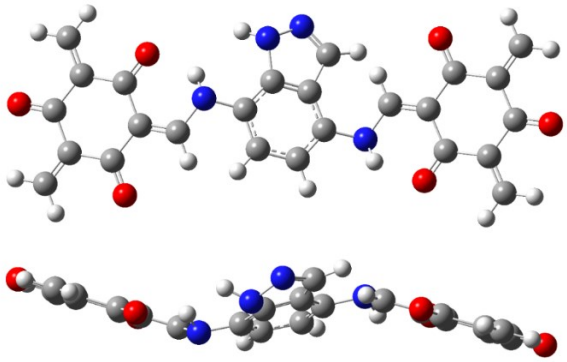

Figure S 14 The optimized structure for COF-DAI-TFB with DFT method (Front and Side View).

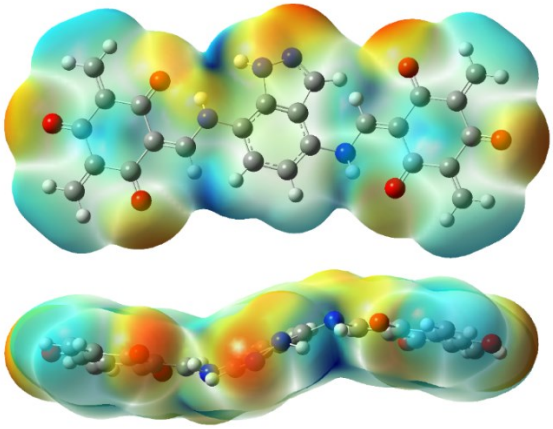

Figure S 15 Electrostatic potential surfaces (ESP) map for the optimized structure for COF-DAI-TFB.

7. Structural modeling and Powder X-Ray Diffraction analysis

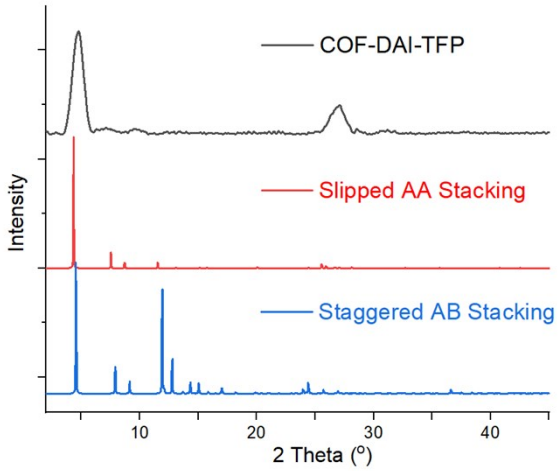

Figure S 16 The XRD pattern of COF-DAI-TFP, and the XRD patterns of its simulated models.

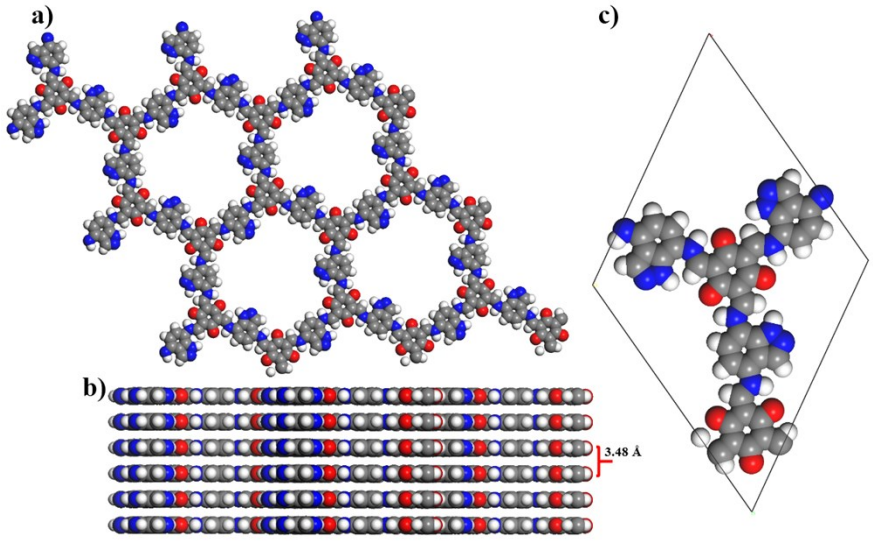

Figure S 17 The a) Top and b) side views of the slipped AA-stacking model of COF-DAI-TFP. c) Units cells of slipped AA-stacking mode of COF-DAI-TFP. (P1m1; a= 23.7, b= 3.5, c= 24.9 Å; α =90.0, β= 124.8, γ=90.0 °)

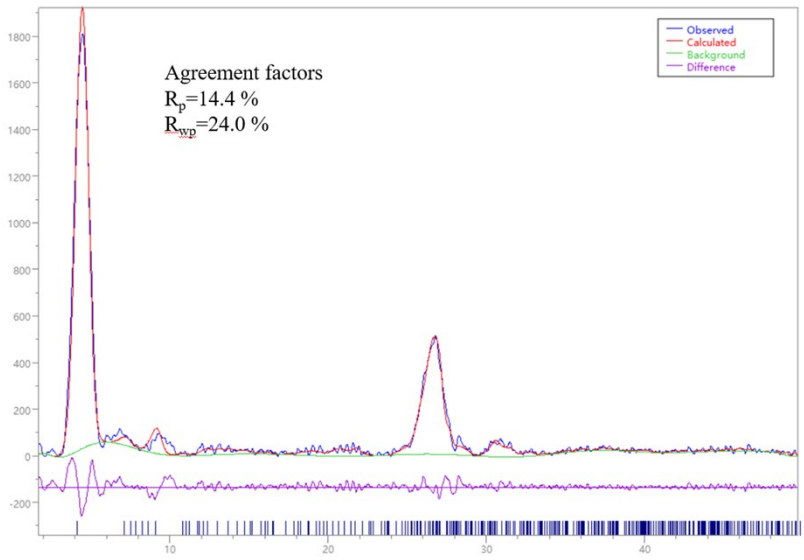

Figure S 18 Comparison of experimental (blue) and simulated (red) PXRD pattern (COF-DAI-TFP in slipped stacking mode). Difference plot is depicted in violet line. Pawley refinement demonstrates good agreement between experimental and slipped AA stacking PXRD pattern (Rwp: 14.4%, Rp: 24.0%).

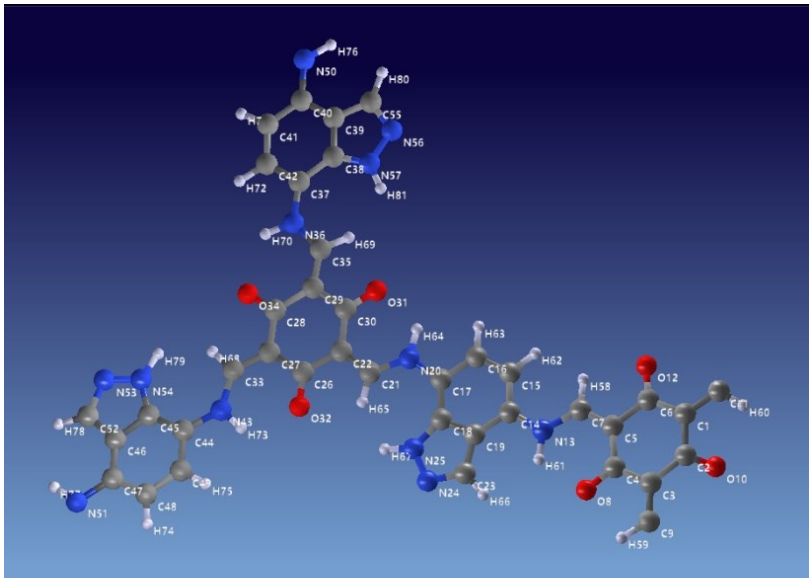

Figure S 19 Unit cell structure of COF-DAI-TFP.

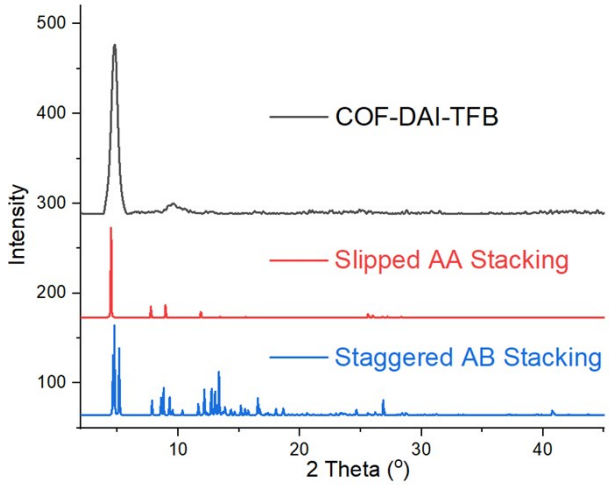

Figure S 20 The XRD pattern of COF-DAI-TFB, and the XRD patterns of its simulated models.

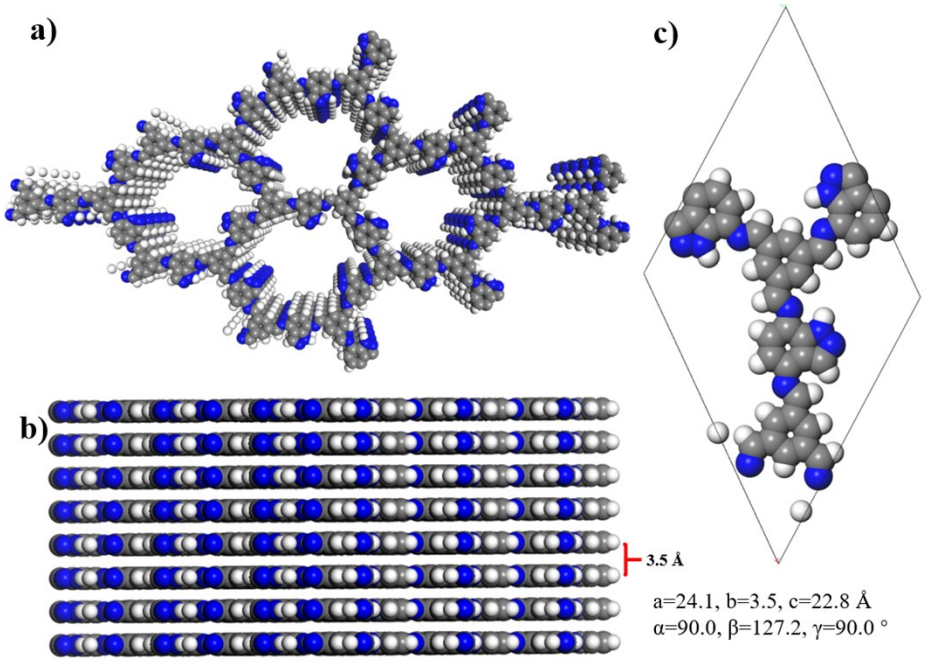

Figure S 21 The a) Top and b) side views of the slipped AA-stacking model of COF-DAI-TFB. c) Units cells of slipped AA-stacking mode of COF-DAI-TFB.(P1m1; a=24.15, b=3.48, c=22.80 Å; α =90.0, β=127.1, γ=90.0 °)

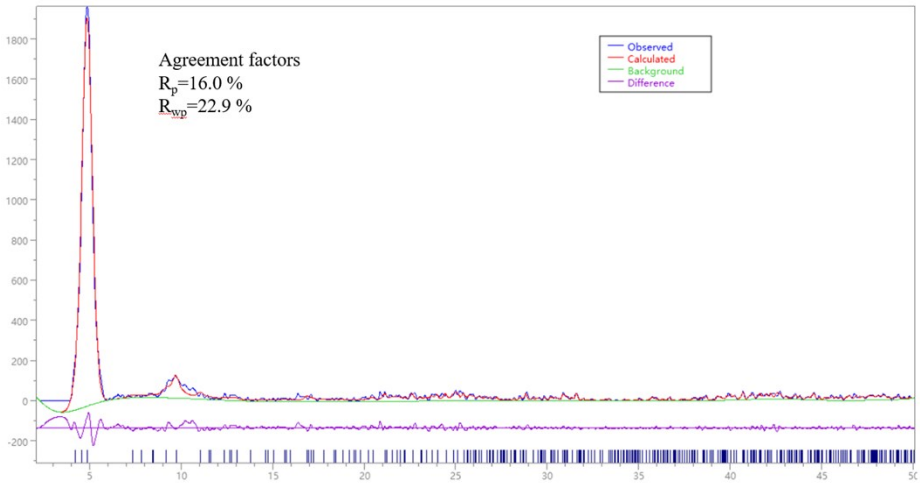

Figure S 22 Comparison of experimental (blue) and simulated (red) PXRD pattern (COF-DAI-TFB in slipped stacking mode). Difference plot is depicted in violet line. Pawley refinement demonstrates good agreement between experimental and slipped AA stacking PXRD pattern (Rwp: 22.9%, Rp: 16%).

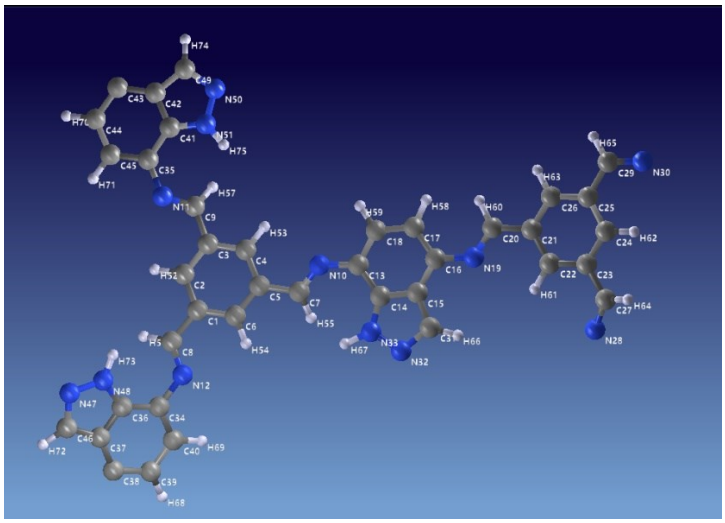

Figure S 23 Unit cell structure of COF-DAI-TFB.

8. Solid-State NMR and FT-IR Spectrum of COF-DAI-TFP and COF-DAI-TFB

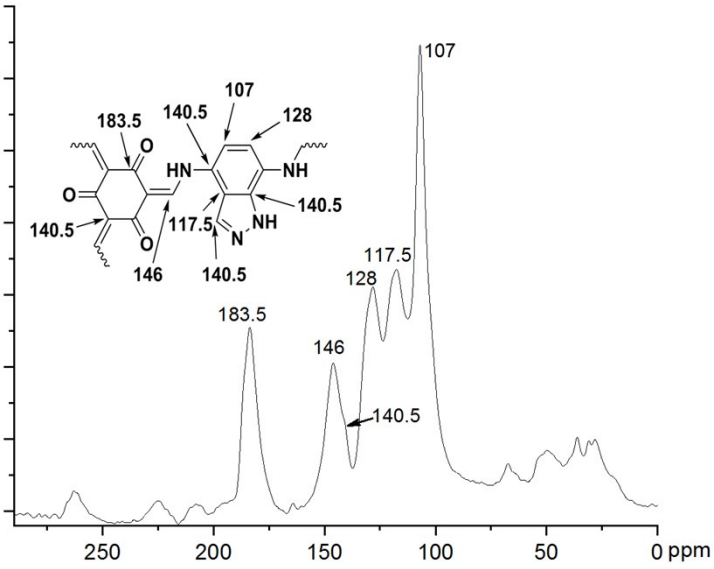

Figure S 24 The ^{13}C Cross-polarization/magic-angle spinning (CP/MAS) solid-state NMR of COF-DAI-TFP.

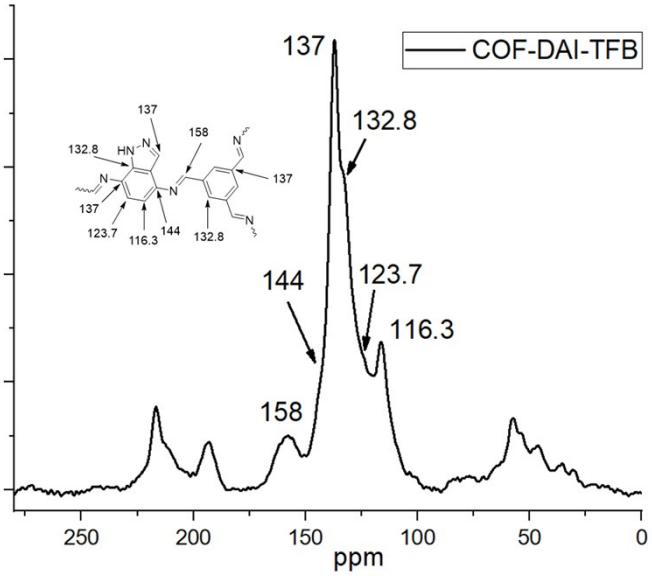

Figure S 25 The ^{13}C Cross-polarization/magic-angle spinning (CP/MAS) solid-state NMR of COF-DAI-TFB.

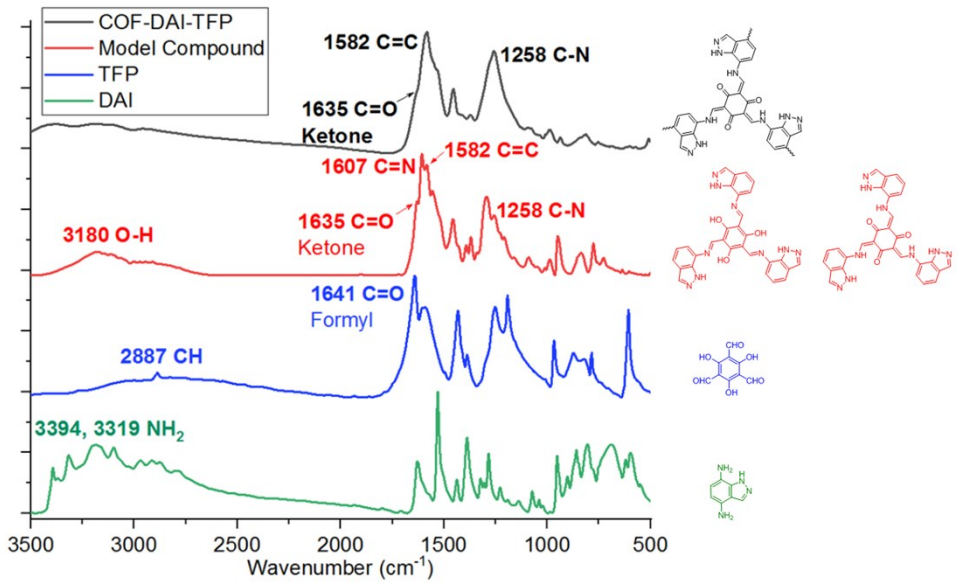

Figure S 26 The TF-IR spectrum of COF-DAI-TFP, and its corresponding monomers and model compound.

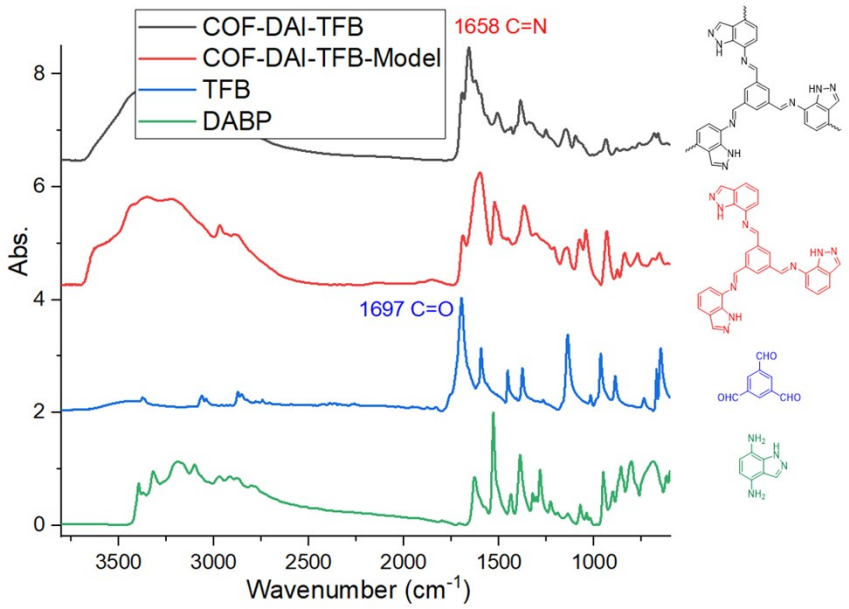

Figure S 27 The TF-IR spectrum of COF-DAI-TFB, and its corresponding monomers and model compound.

9. N2 Adsorption-Desorption Analysis of COF-DAI-TFP

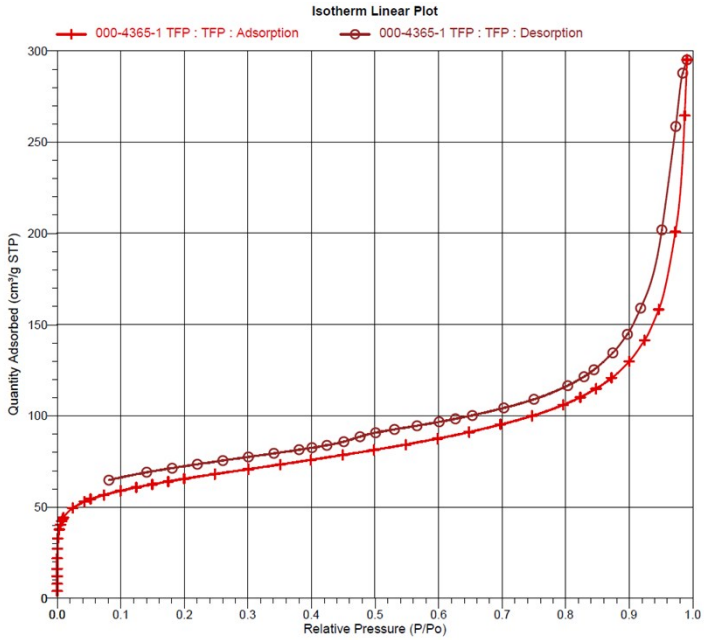

Figure S 28 The nitrogen sorption isotherm of COF-DAI-TFP at 77K (236.2 m^2 g^{-1}).

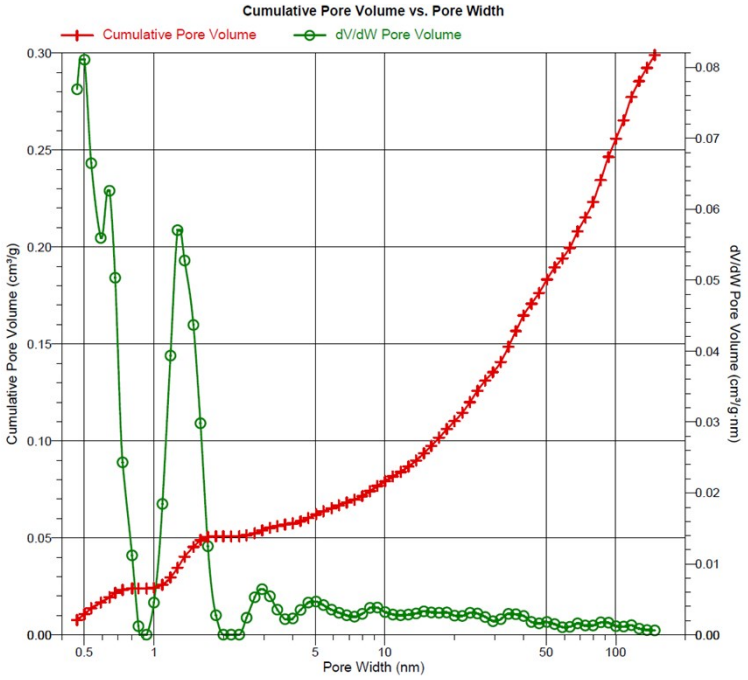

Figure S 29 The pore width dispersion of COF-DAI-TFP (Calculated by NLDFT slit pores model).

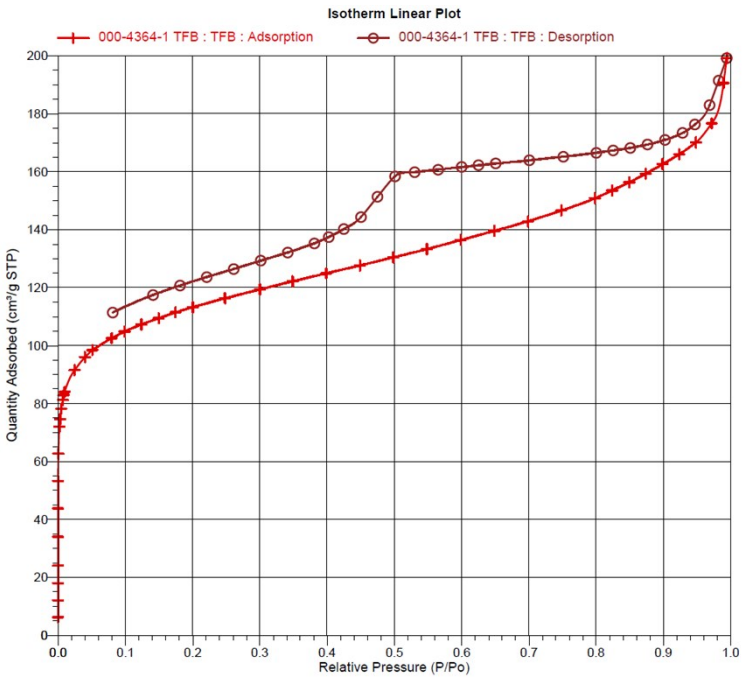

Figure S 30 The nitrogen sorption isotherm of COF-DAI-TFB at 77K (417.4 $m^2 g^{-1}$).

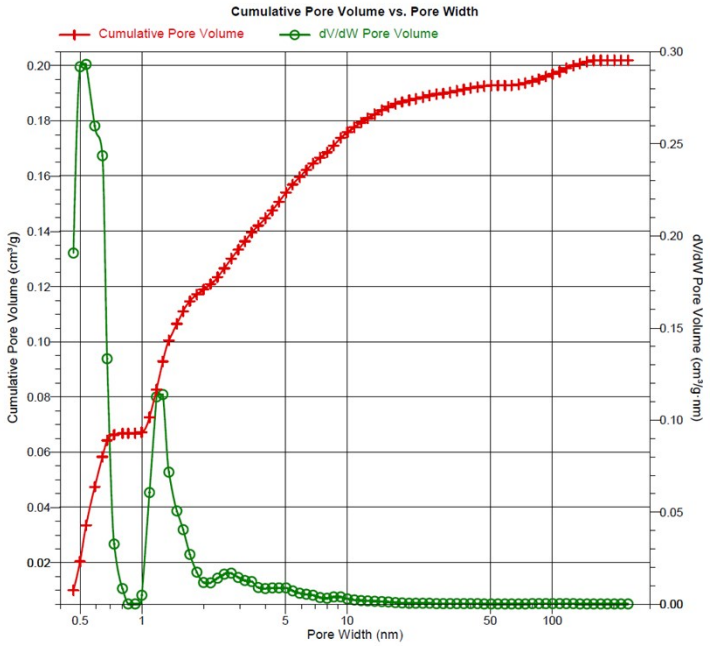

Figure S 31 The pore width dispersion of COF-DAI-TFB (Calculated by NLDFT slit pores model).

10. Thermogravimetric Analysis of COF-DAI-TFP

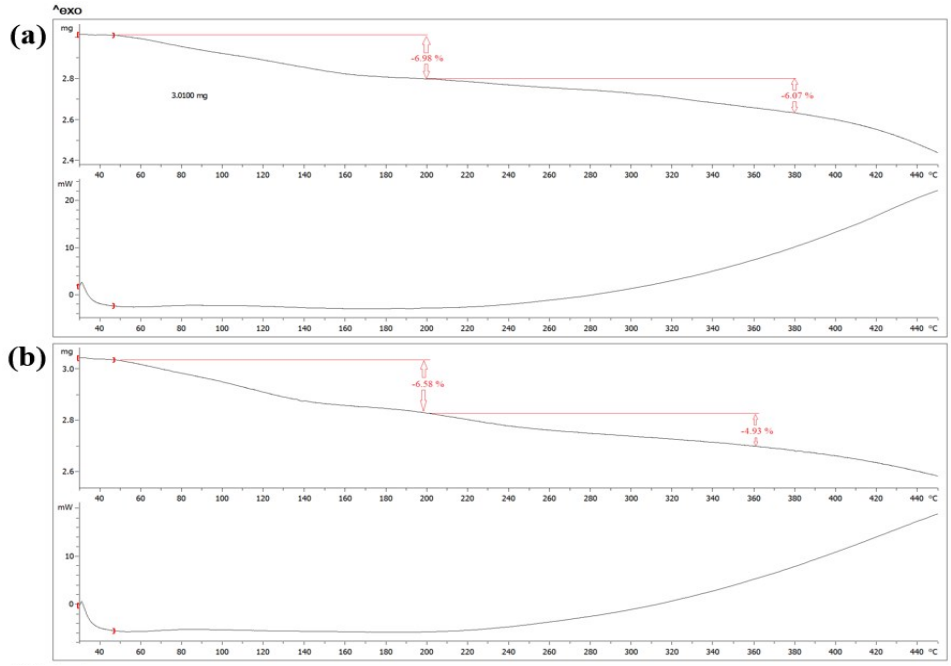

Figure S 32 The thermostability analysis of (a) COF-DAI-TFP and (b) COF-DAI-TFB. (The weight loss before 200 °C can be assigned to the evaporation of high boiling point solvent, because the DSC plot before 200 °C show broad endothermal peak)

11. SEM of COF-DAI-TFP

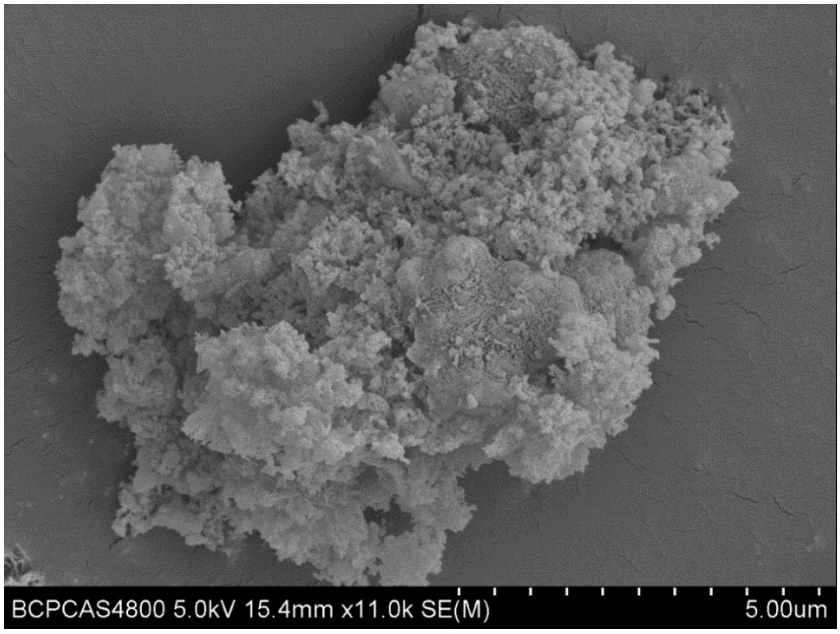

Figure S 33 The low magnification SEM images of COF-DAI-TFP.

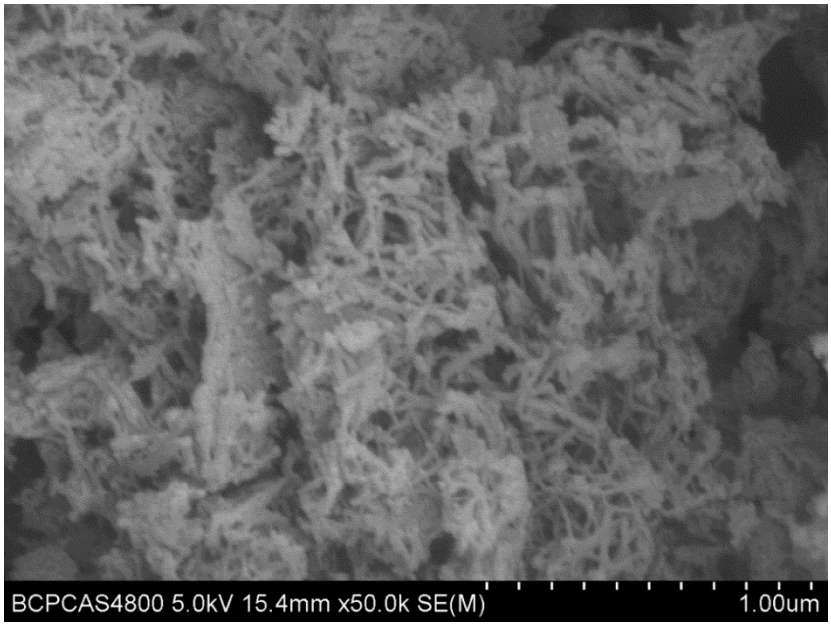

Figure S 34 The high magnification SEM images of COF-DAI-TFP.

12. TEM of COF

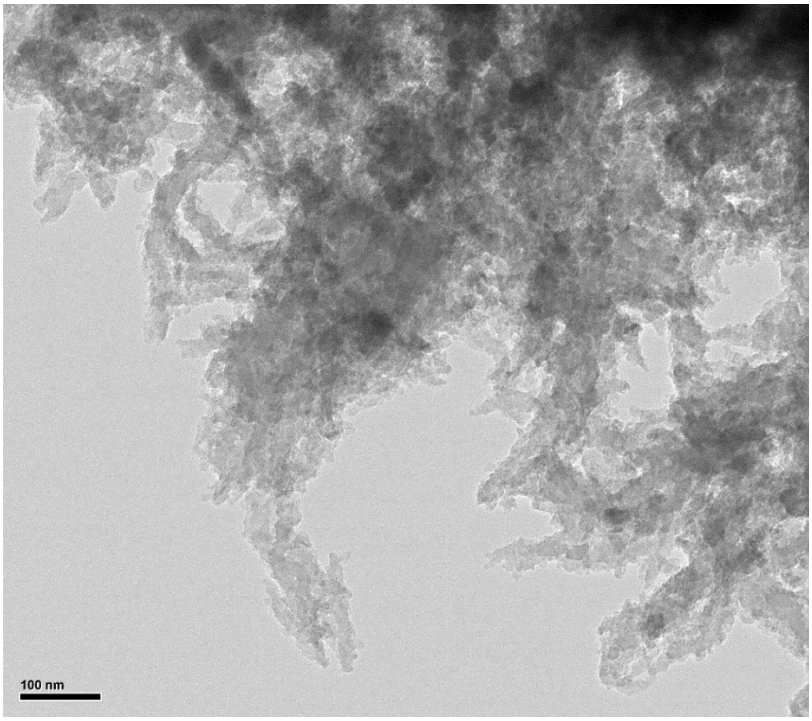

Figure S 35 The low magnification HR-TEM images of COF-DAI-TFP.

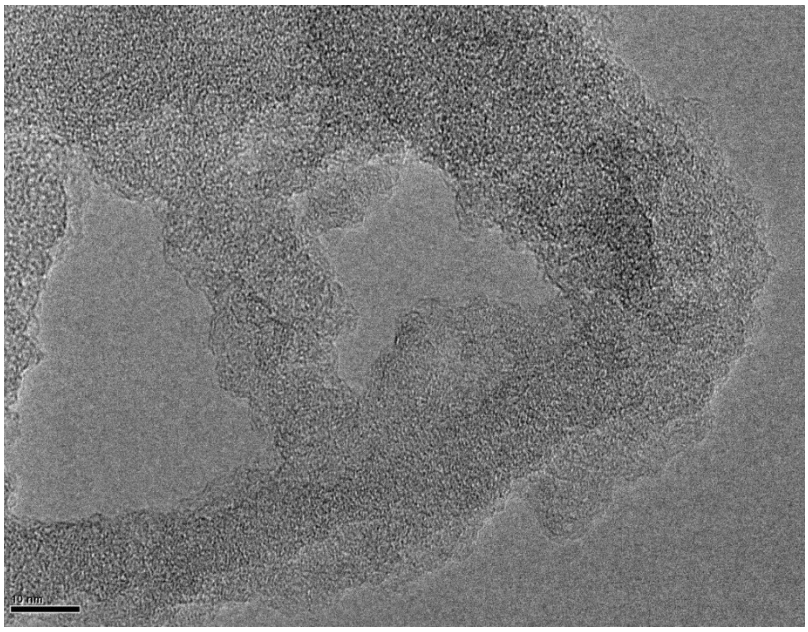

Figure S 36 The high magnification HR-TEM images of COF-DAI-TFP.

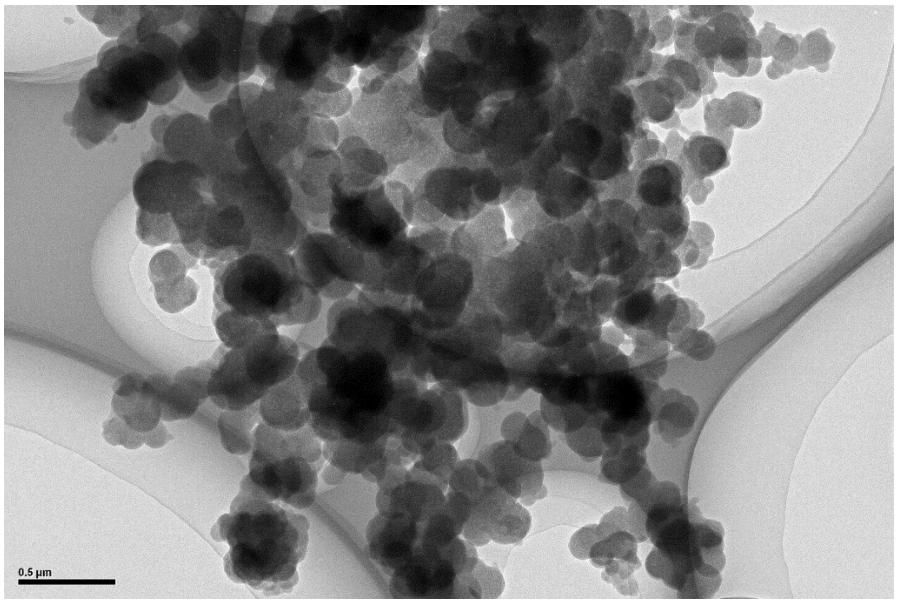

Figure S 37 The HR-TEM images of COF-DAI-TFB.

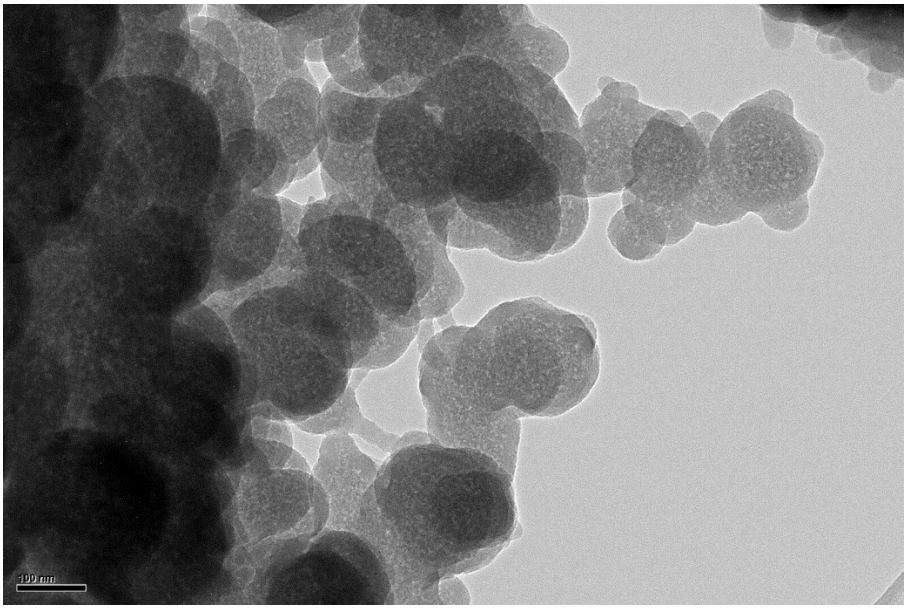

Figure S 38 The HR-TEM images of COF-DAI-TFB.

13. AFM of COF-DAI-TFP

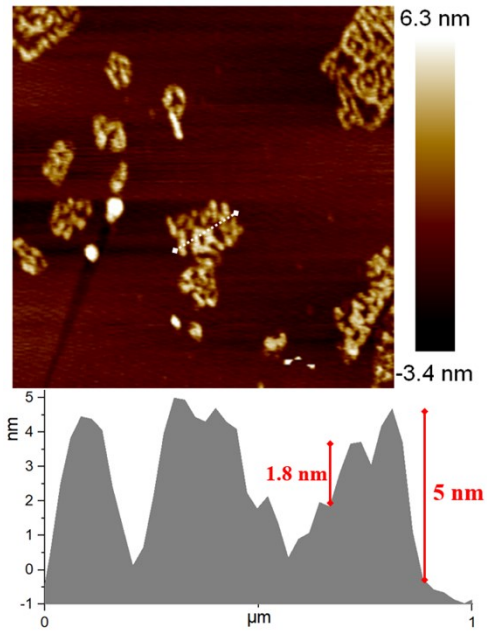

Figure S 39 The AFM images of COF-DAI-TFP.

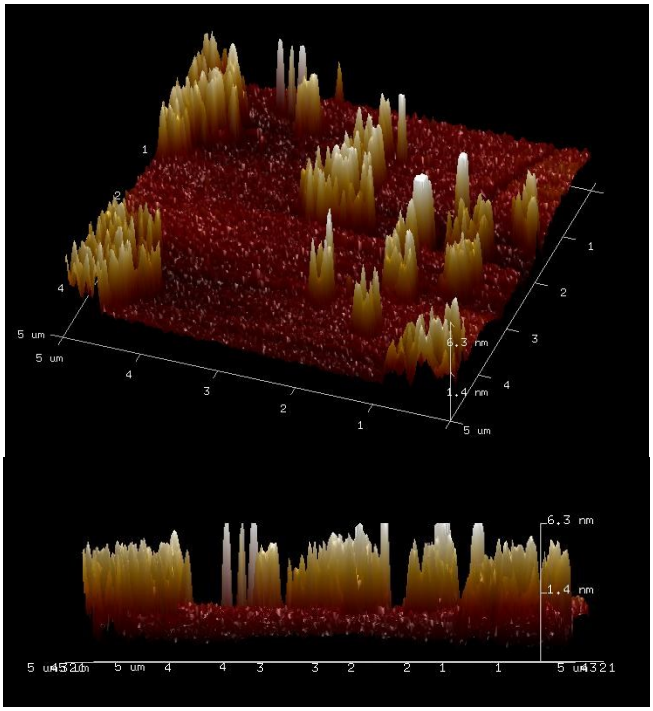

Figure S 40 The oblique and side view AFM images of COF-DAI-TFP.

14. TEM of M@COF

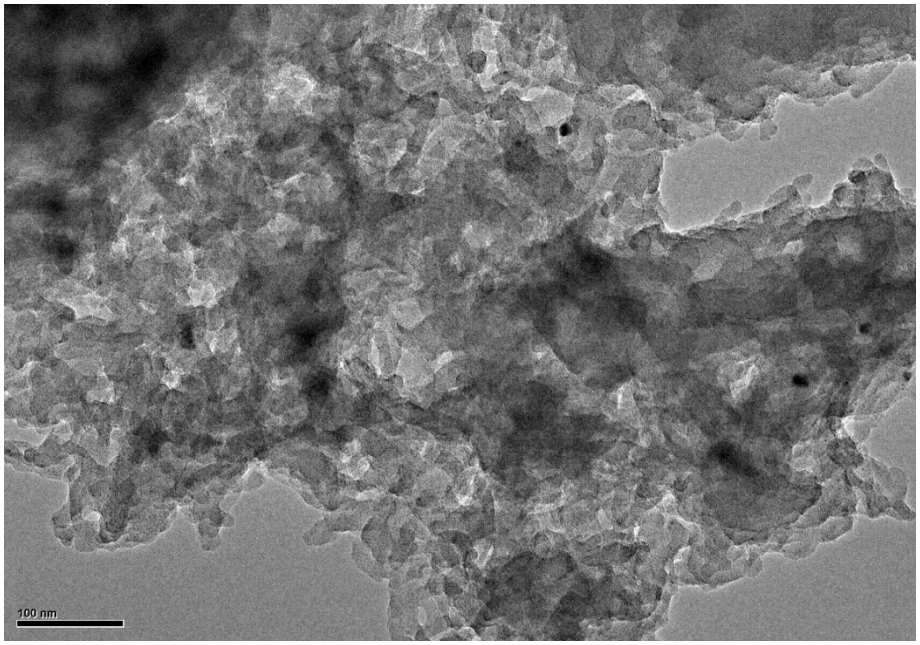

Figure S 41 The low magnification HR-TEM image of Pd@COF-DAI-TFP with high metal content.

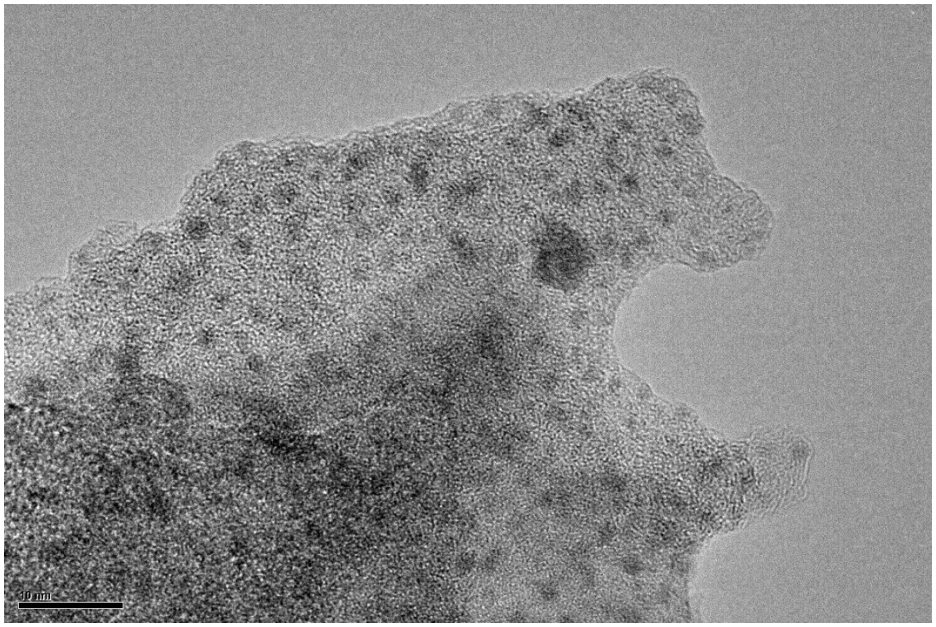

Figure S 42 The high magnification HR-TEM image of Pd@COF-DAI-TFP with high metal content.

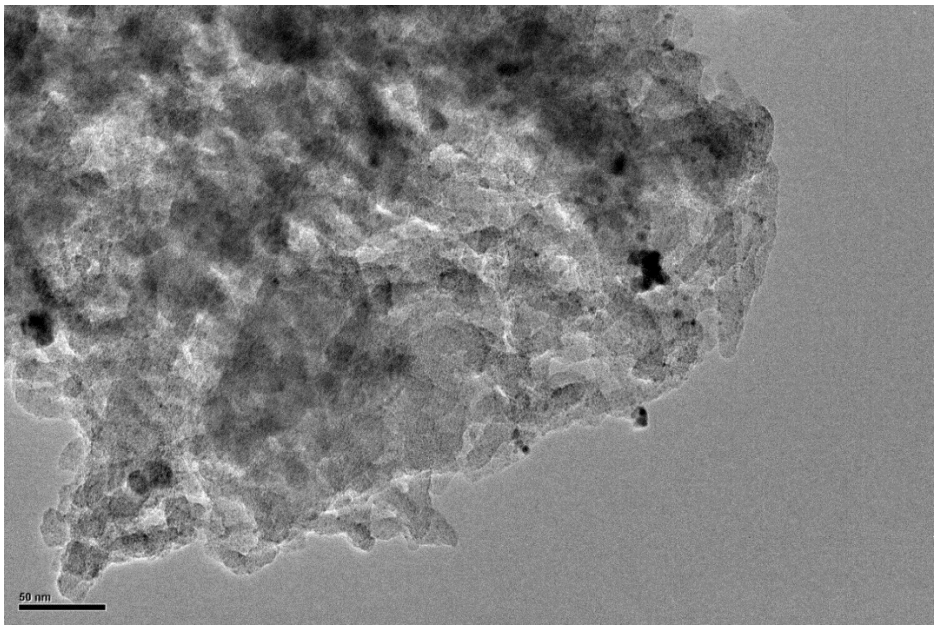

Figure S 43 The low magnification HR-TEM image of the dated (exposure to air for 50 days) Pd@COF-DAI-TFP (high metal content).

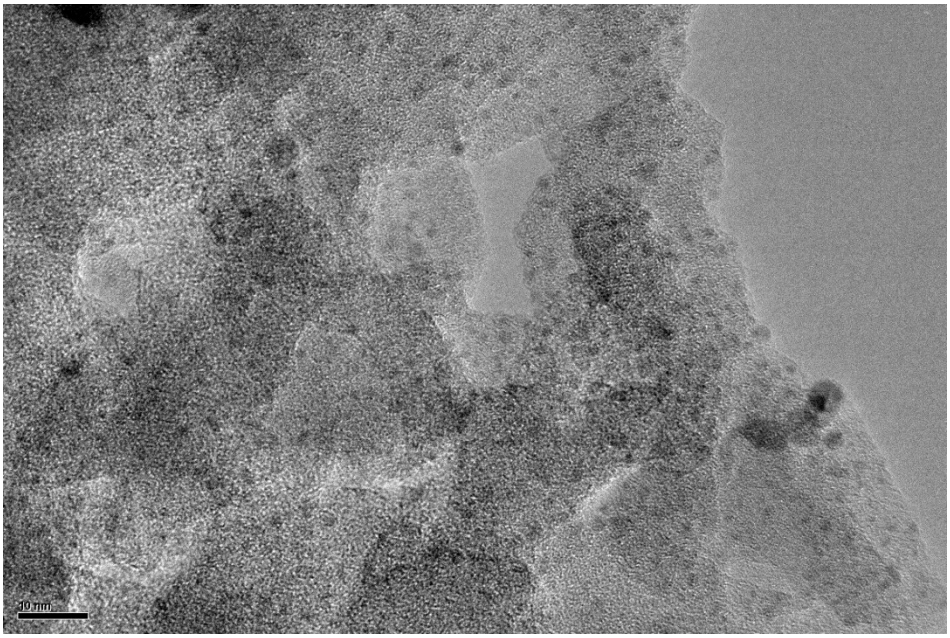

Figure S 44 The high magnification HR-TEM image of the dated (exposure to air for 50 days) Pd@COF-DAI-TFP (high metal content).

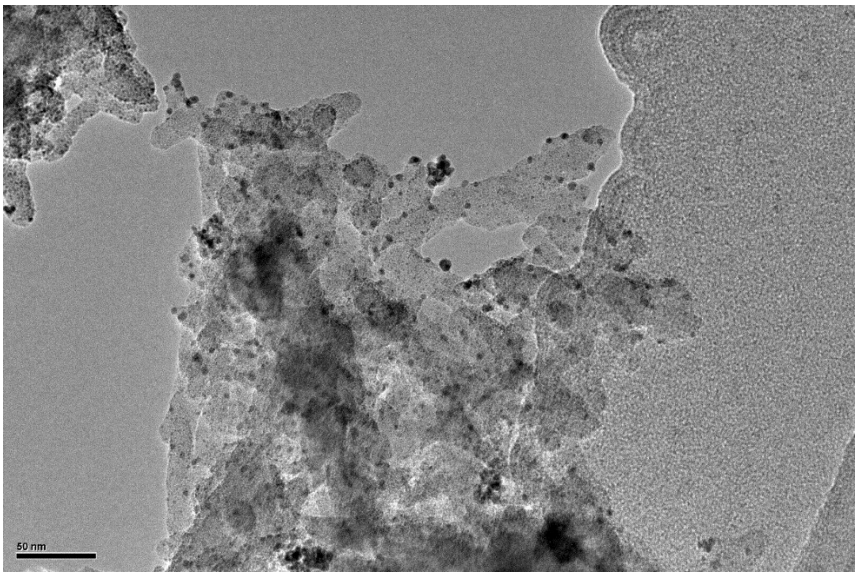

Figure S 45 The low magnification HR-TEM image of the dated (exposure to air for 50 days) Pd@COF-DAI-TFP (high metal content) after used for 5 times in the *p*-nitrophenol reduction reaction.

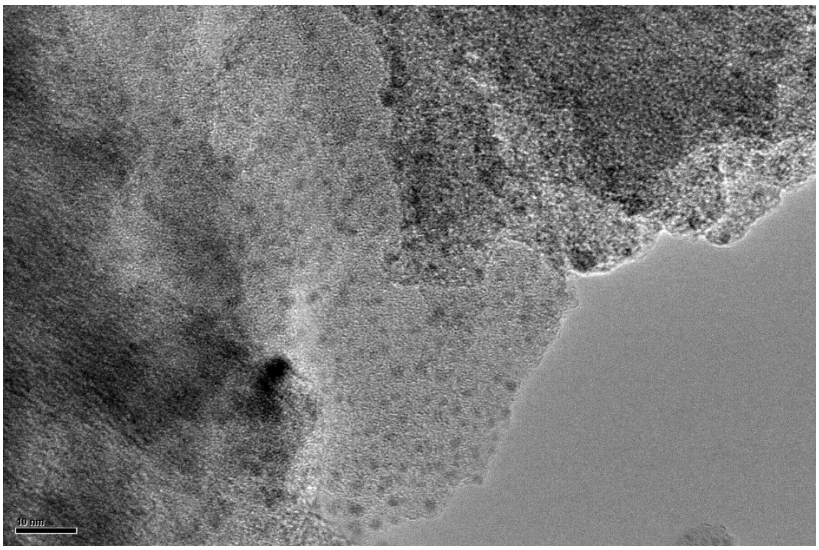

Figure S 46 The high magnification HR-TEM image of the dated (exposure to air for 50 days) Pd@COF-DAI-TFP (high metal content) after used for 5 times in the *p*-nitrophenol reduction reaction.

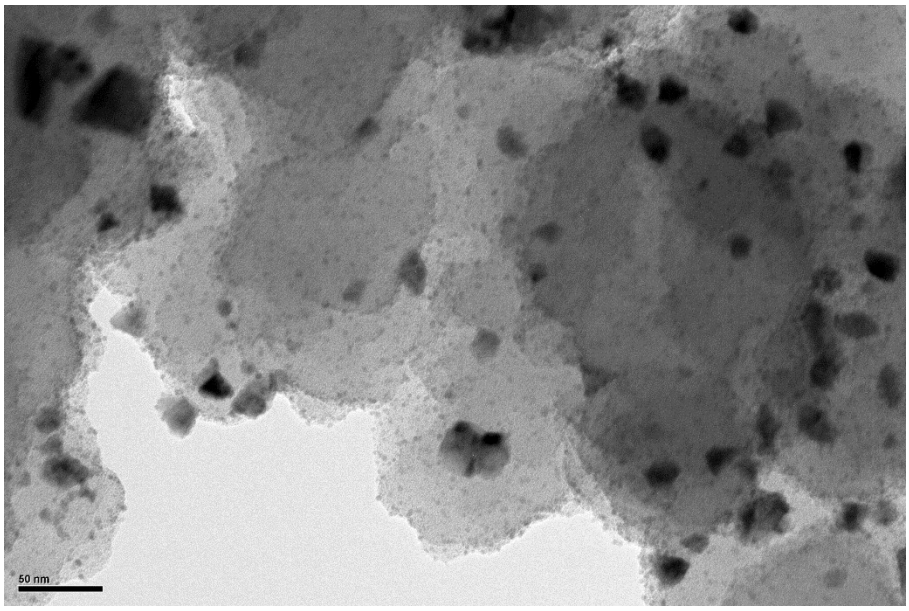

Figure S 47 The low magnification HR-TEM image of Pd@COF-DAI-TFB with high metal content.

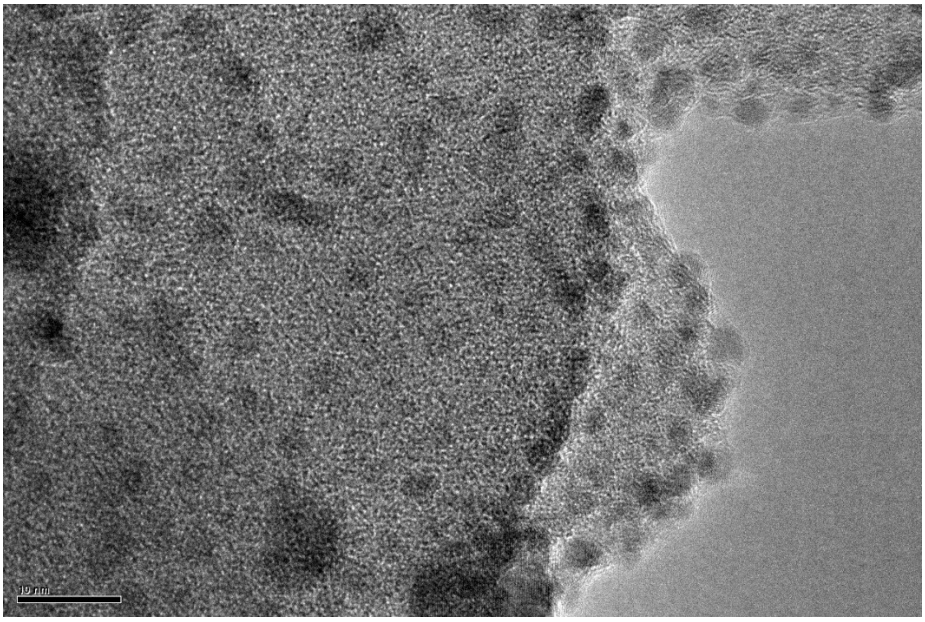

Figure S 48 The high magnification HR-TEM image of Pd@COF-DAI-TFB with high metal content.

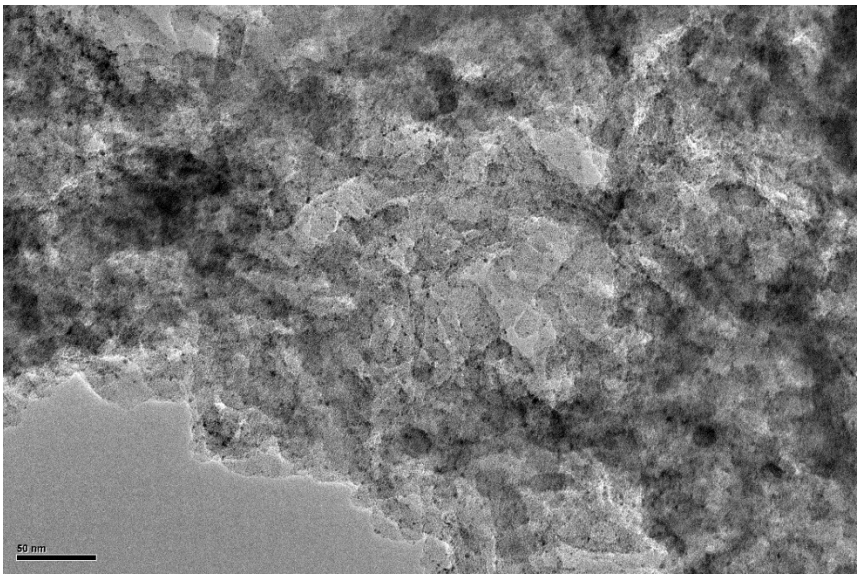

Figure S 49 The low magnification HR-TEM image of Ir@COF-DAI-TFP with high metal content.

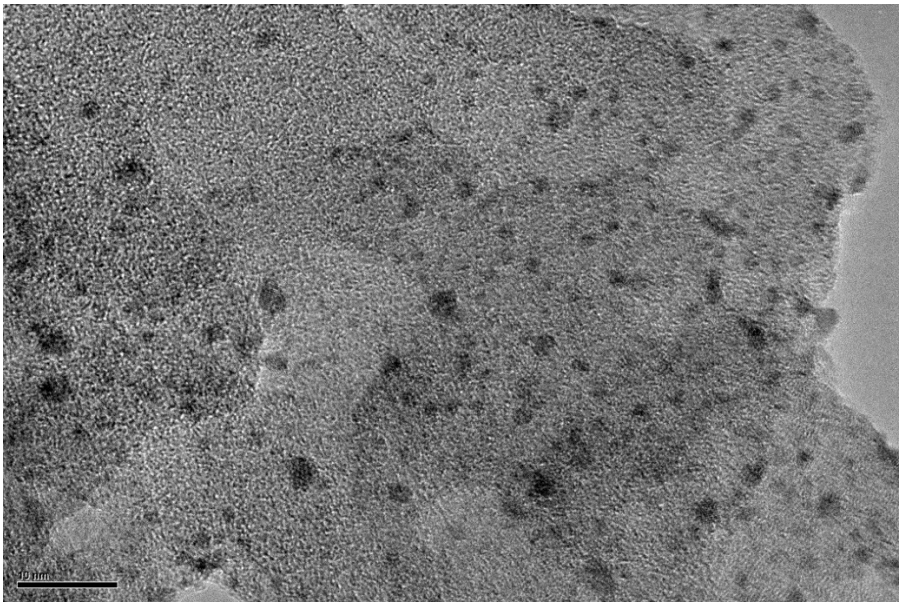

Figure S 50 The high magnification HR-TEM image of Ir@COF-DAI-TFP with high metal content.

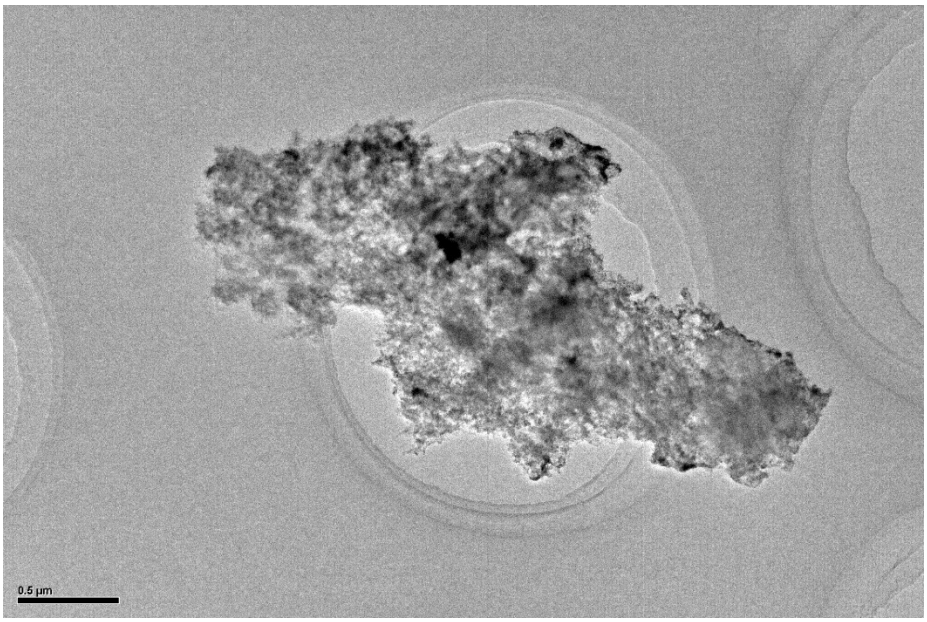

Figure S 51 The low magnification HR-TEM image of Pt@COF-DAI-TFP with high metal content.

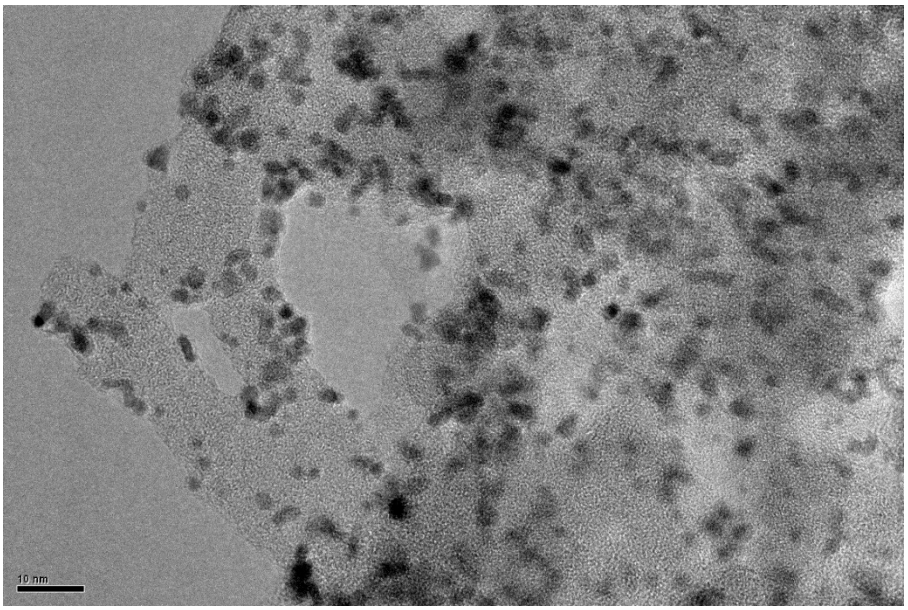

Figure S 52 The high magnification HR-TEM image of Pt@COF-DAI-TFP with high metal content.

15. Energy Dispersive Spectroscope (EDS) Mapping Scan of M@COF-DAI-TFP

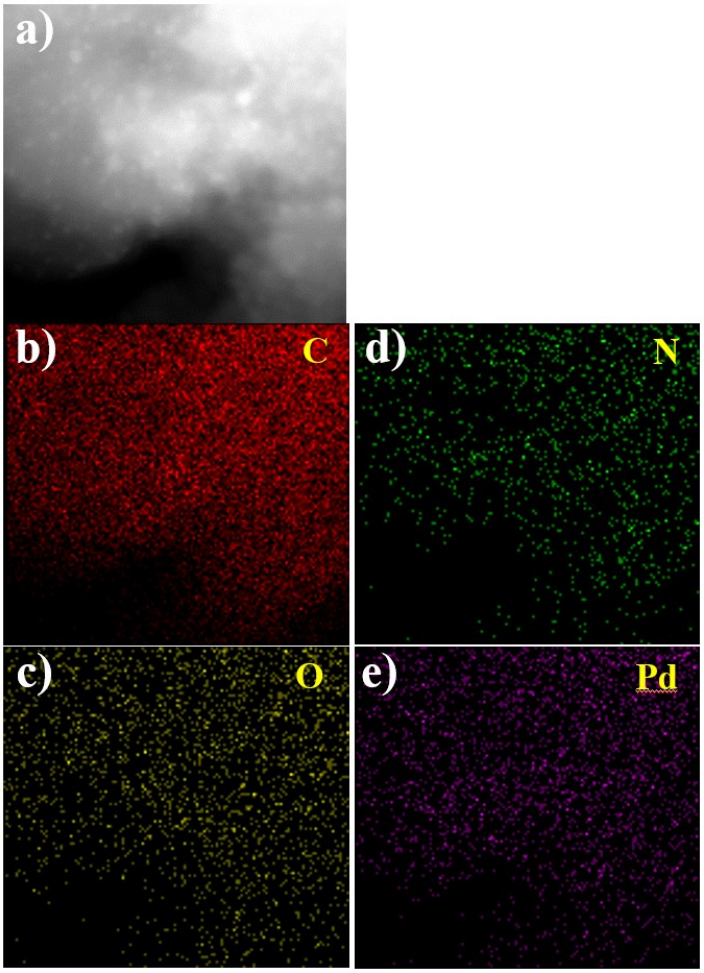

Figure S 53 EDS mapping scan of Pd@COF-DAI-TFP.

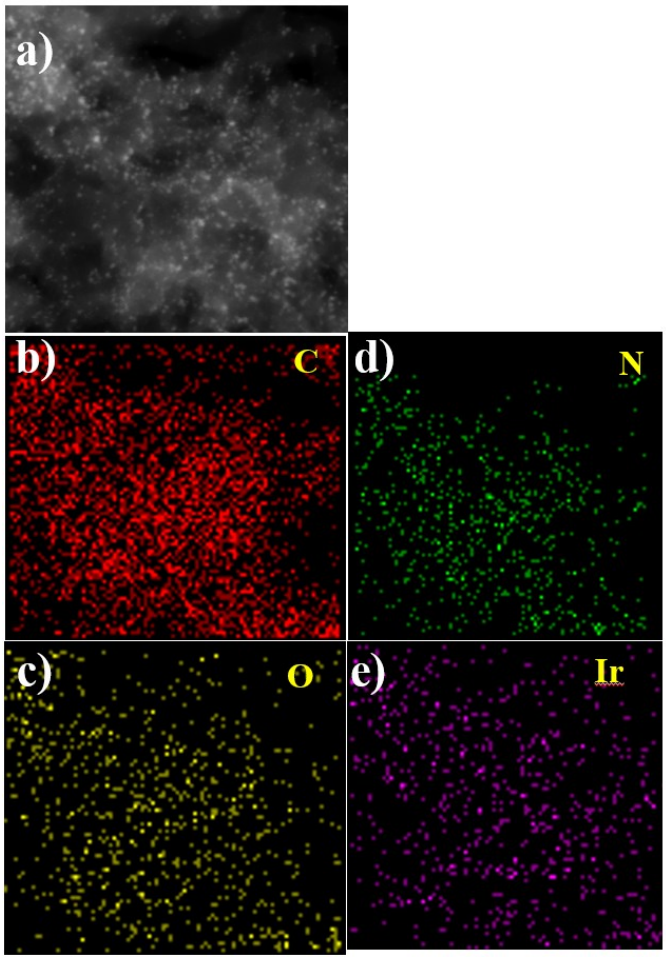

Figure S 54 EDS mapping scan of Ir@COF-DAI-TFP.

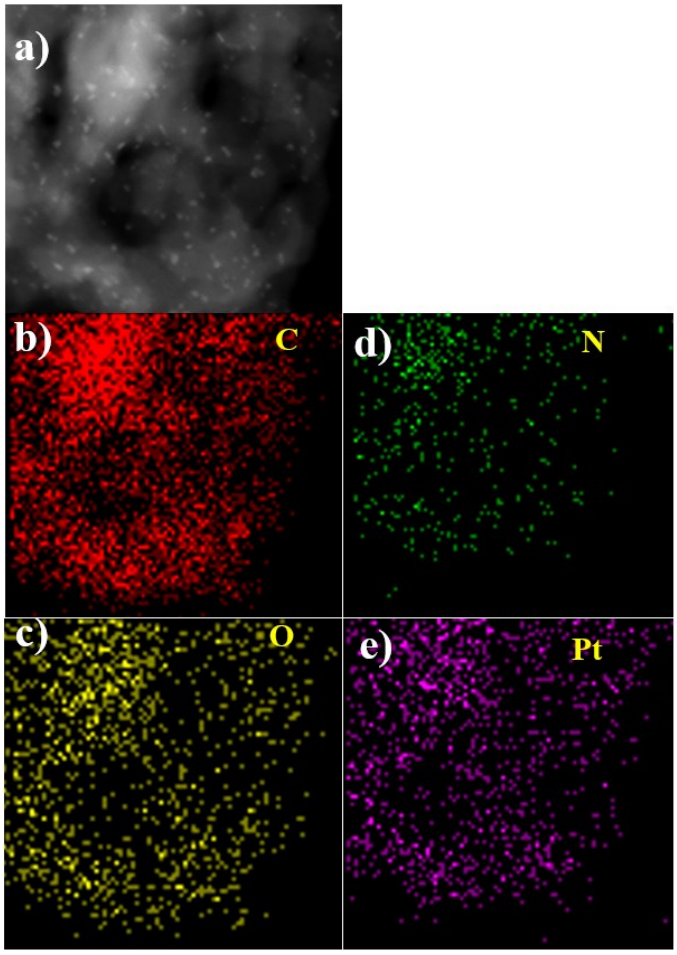

Figure S 55 EDS mapping scan of Pt@COF-DAI-TFP.

16. Metal particle width dispersion of M@COF-DAI-TFP

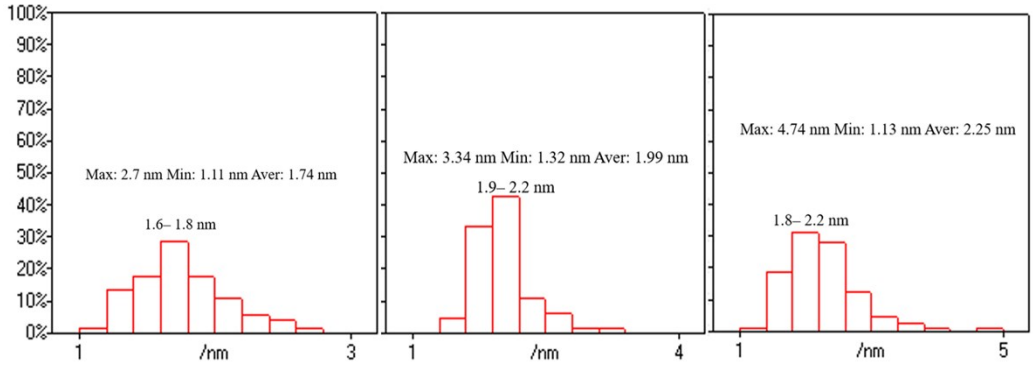

Figure S 56 The particle width dispersion of Pd@COF-DAI-TFP, Ir@COF-DAI-TFP and Pt@COF-DAI-TFP

17. Interplanar spacing of metal NPs on COF-DAI-TFP

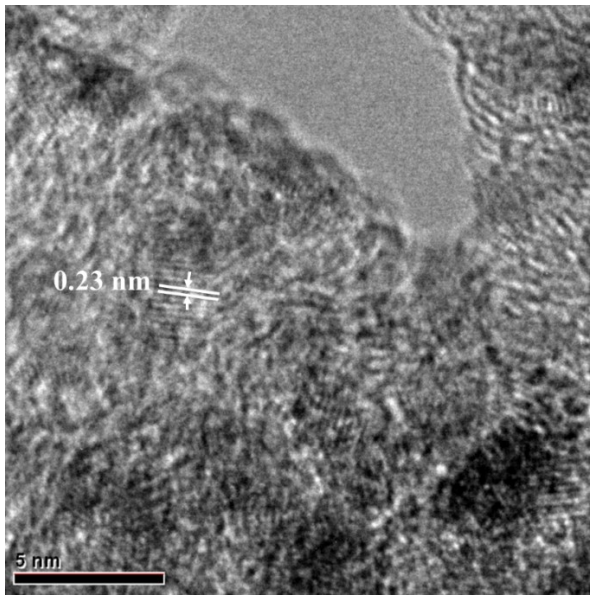

Figure S 57 Interplanar spacing of Pd NMNPs in Pd@COF-DAI-TFP.

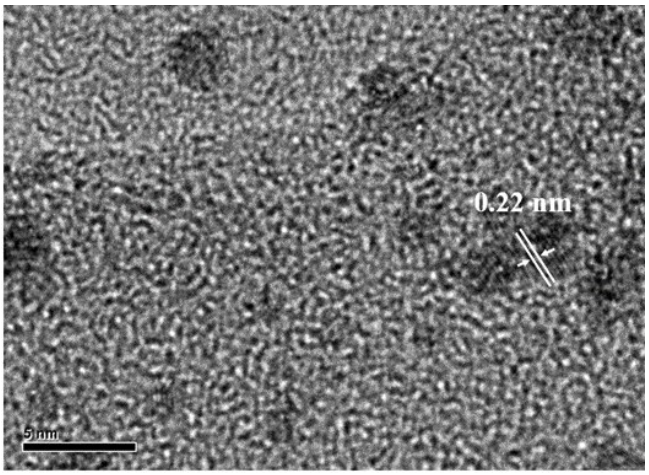

Figure S 58 Interplanar spacing of Ir NMNPs in Ir@COF-DAI-TFP.

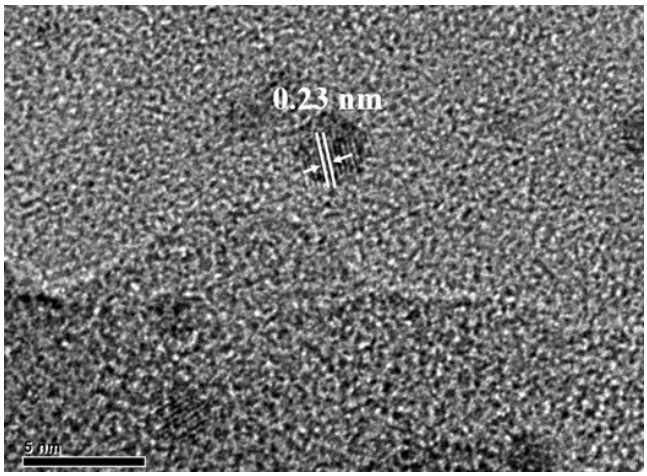

Figure S 59 Interplanar spacing of Pt NMNPs in Pt@COF-DAI-TFP.

18. Selected area electron diffraction (SAED) patterns of M@COF-DAI-TFP

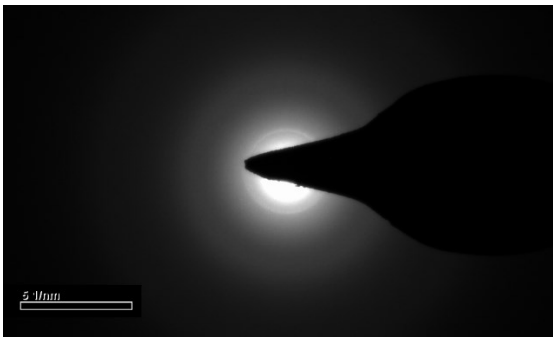

Figure S 60 The SAED pattern of Pd@COF-DAI-TFP.

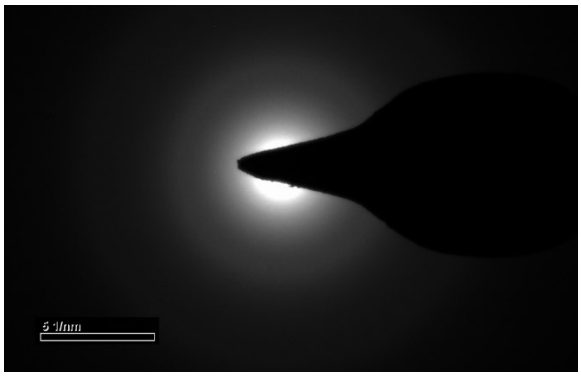

Figure S 61 The SAED pattern of Ir@COF-DAI-TFP.

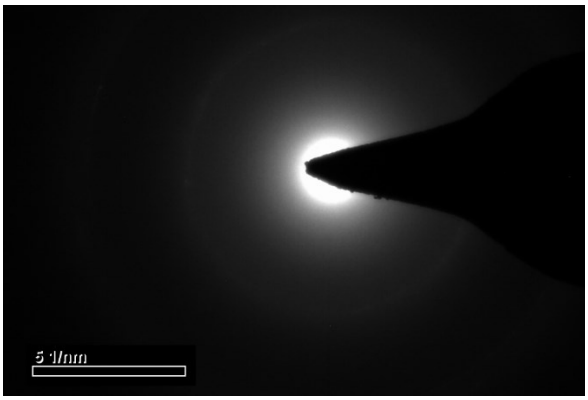

Figure S 62 The SAED pattern of Pt@COF-DAI-TFP.

19. XRD of M@COF-DAI-TFP

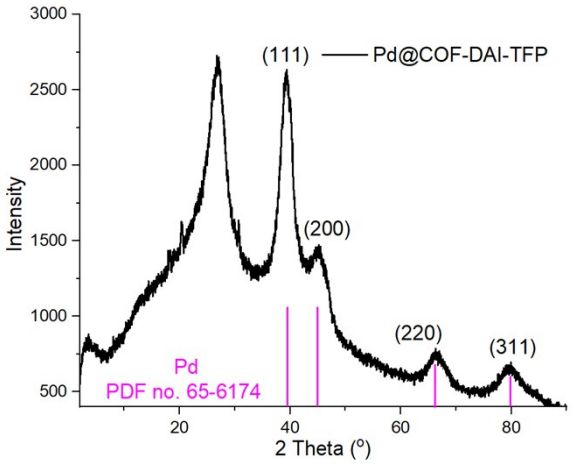

Figure S 63 The PXRD image of Pd@COF-DAI-TFP.

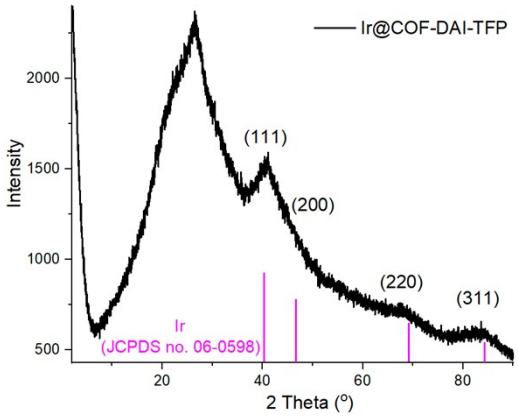

Figure S 64 The PXRD image of Ir@COF-DAI-TFP.

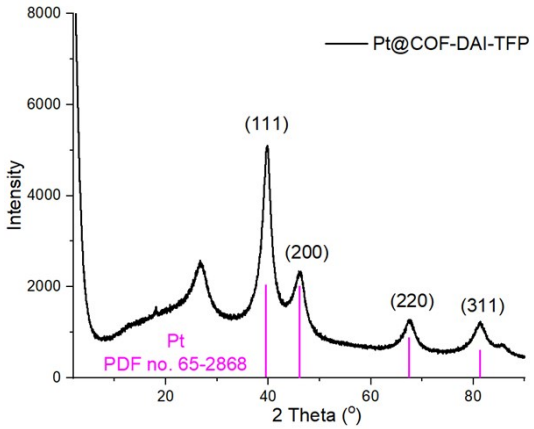

Figure S 65 The PXRD image of Pt@COF-DAI-TFP.

20. SEM of M@COF-DAI-TFP

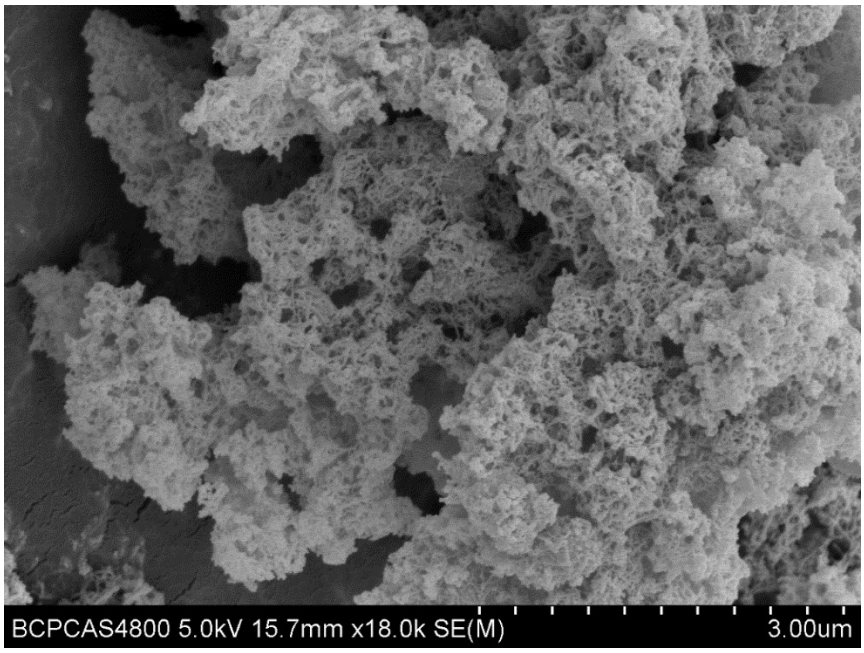

Figure S 66 The SEM images of Pd@COF-DAI-TFP with high metal content.

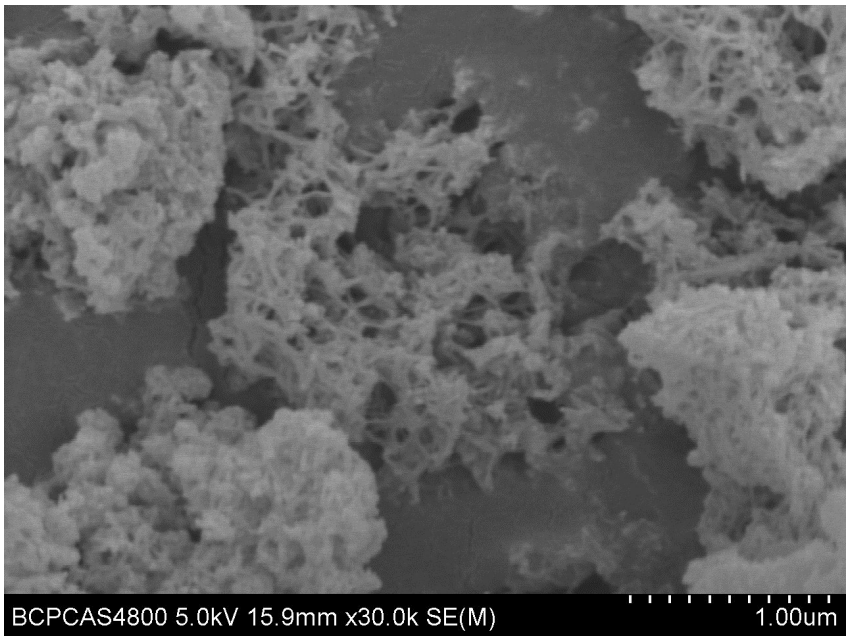

Figure S 67 The SEM images of Ir@COF-DAI-TFP with high metal content.

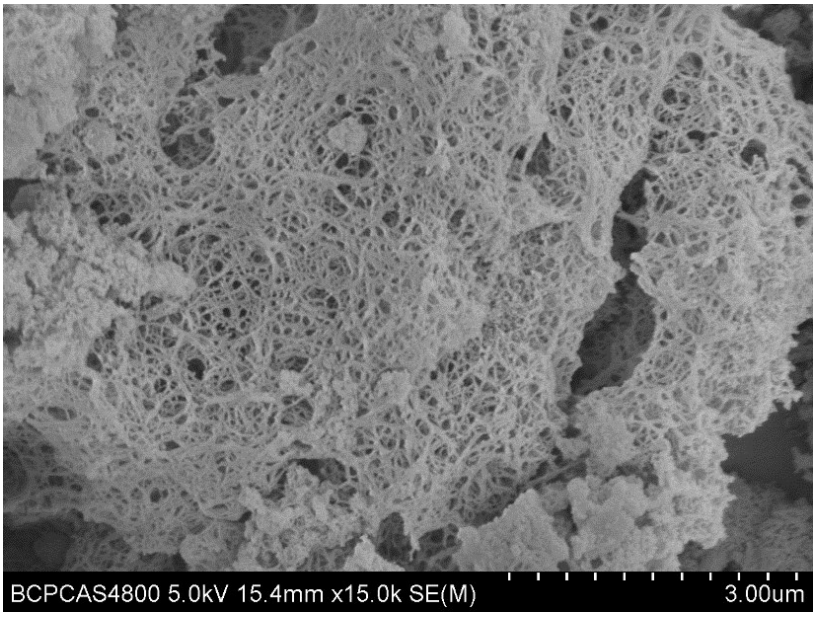

Figure S 68 The HR-TEM images of Pt@COF-DAI-TFP with high metal content.

21. FT-IR of M@COF-DAI-TFP

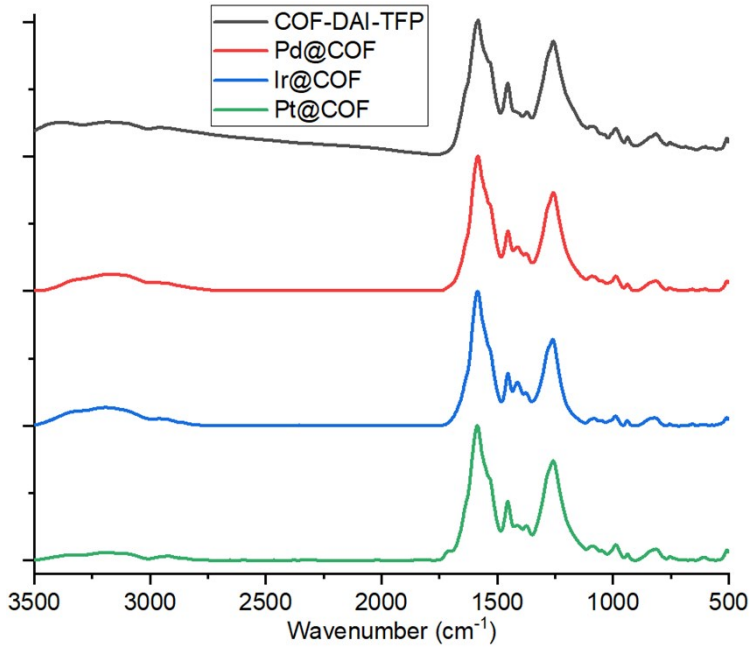

Figure S 69 The FT-IR spectra of M@COF-DAI-TFP.

22. XPS of M@COF-DAI-TFP

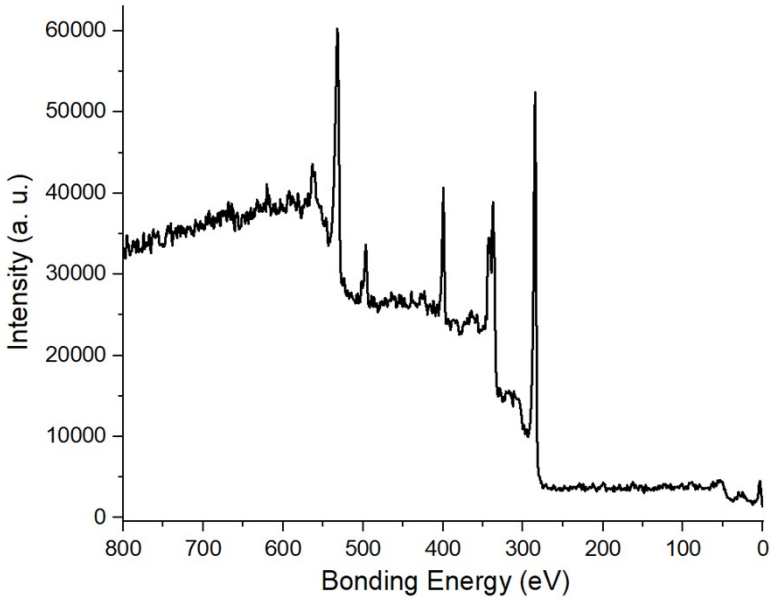

Figure S 70 Full spectrum scan of X-ray photoelectron spectra for Pd@COF-DAI-TFP

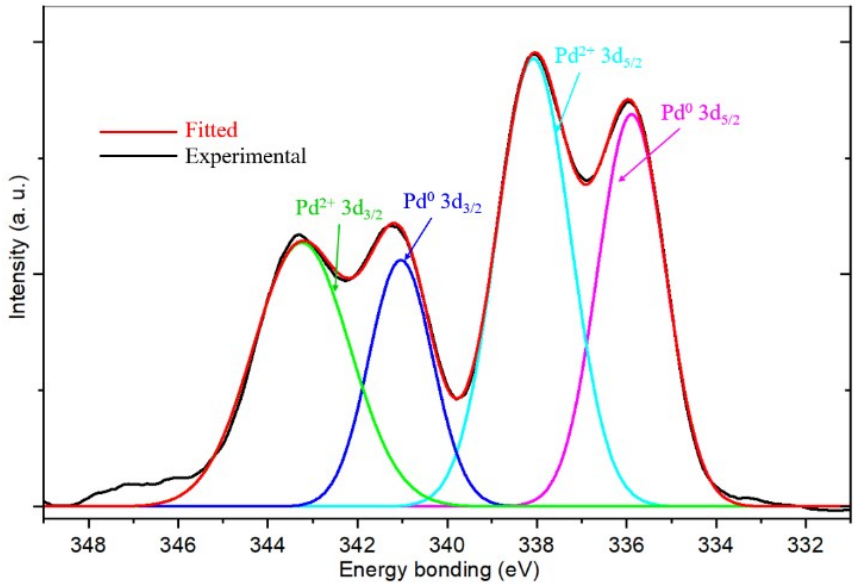

Figure S 71 The Pd 3d region in the XPS spectra of Pd@COF-DAI-TFP.

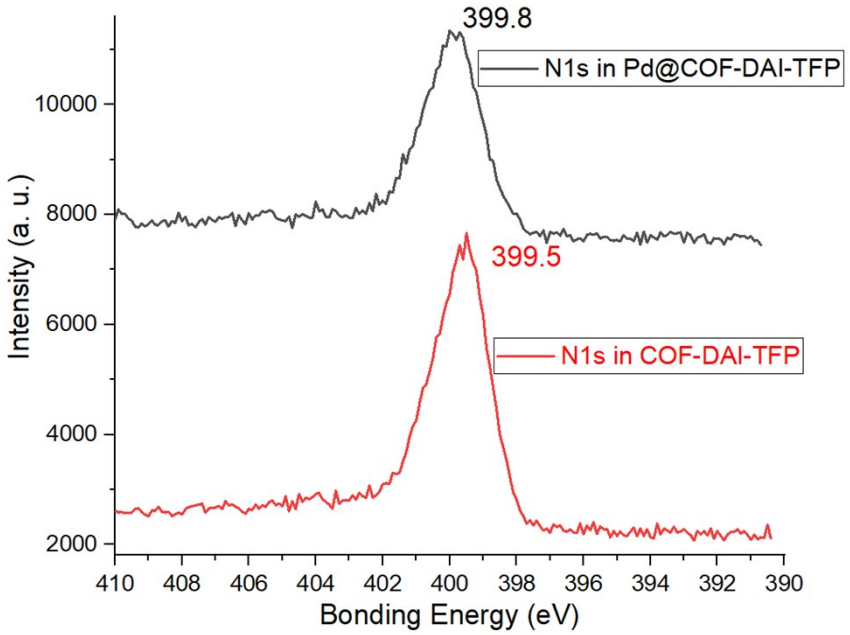

Figure S 72 The N 1S region in the XPS spectra of Pd@COF-DAI-TFP.

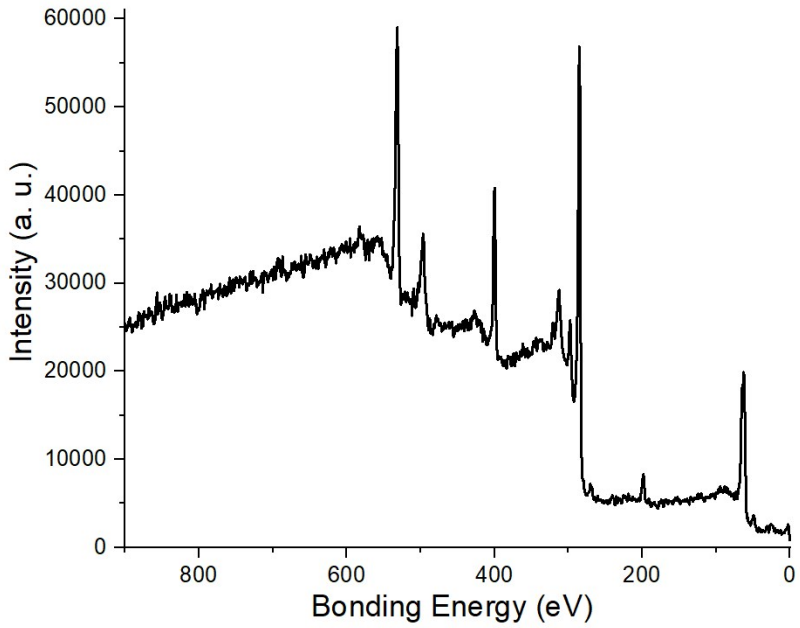

Figure S 73 Full spectrum scan of X-ray photoelectron spectra for Ir@COF-DAI-TFP

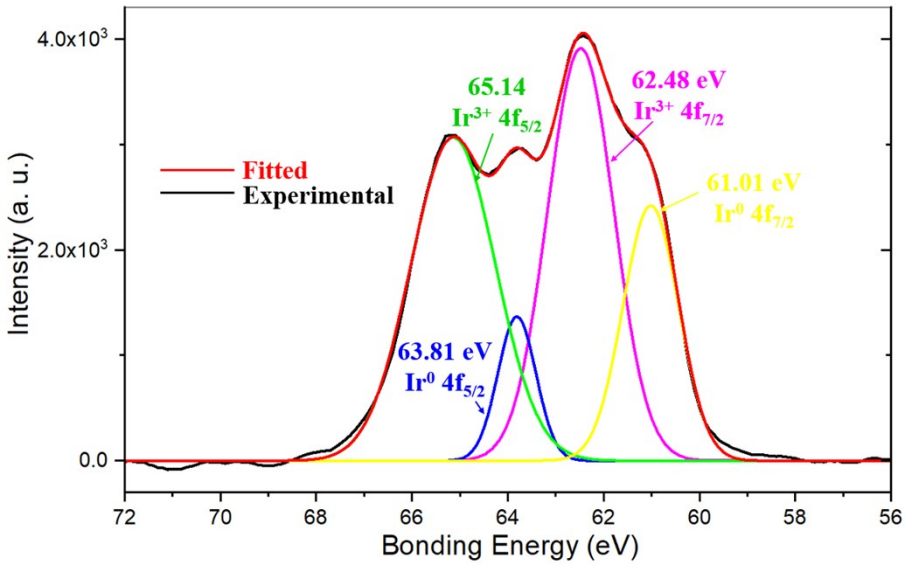

Figure S 74 The Ir 4f region in the XPS spectra of Ir@COF-DAI-TFP.

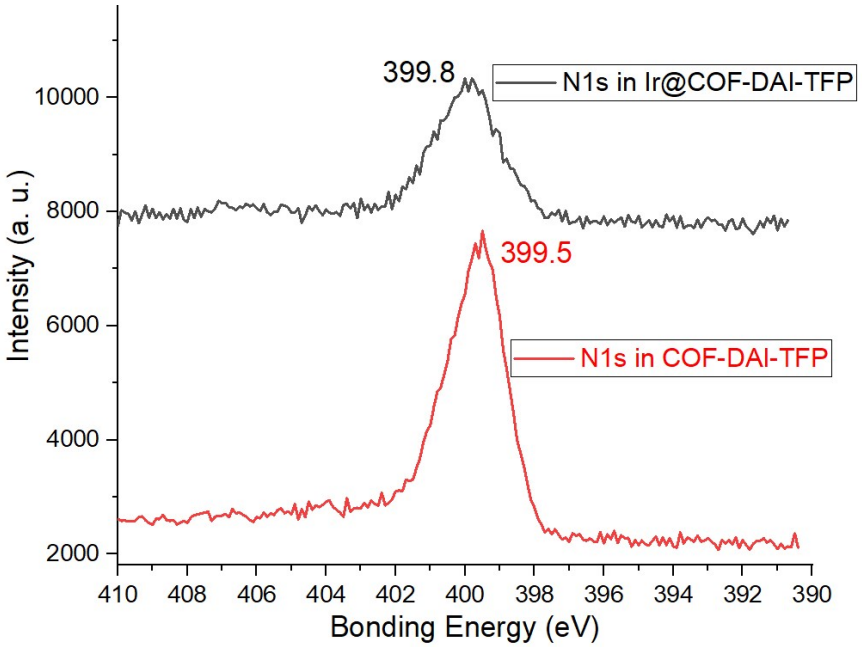

Figure S 75 The N 1S region in the XPS spectra of Ir@COF-DAI-TFP.

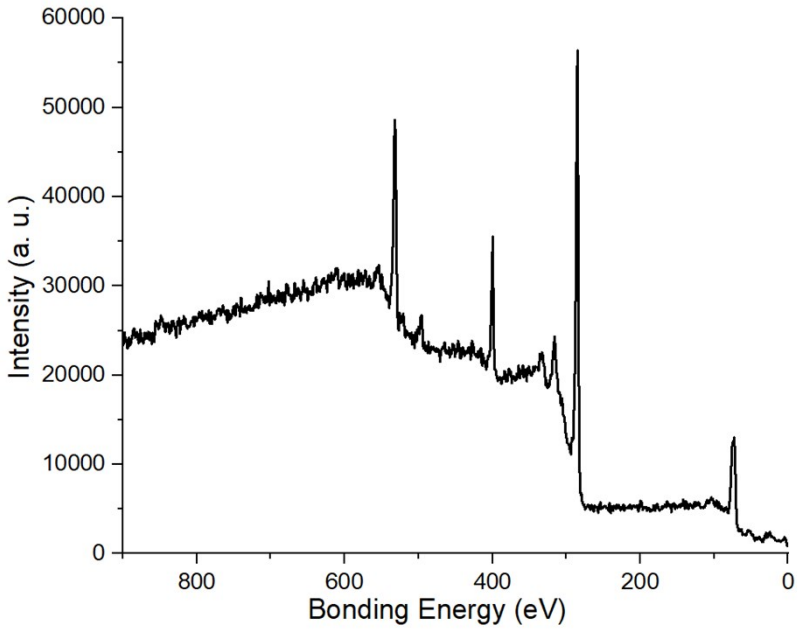

Figure S 76 Full spectrum scan of X-ray photoelectron spectra for Pt@COF-DAI-TFP

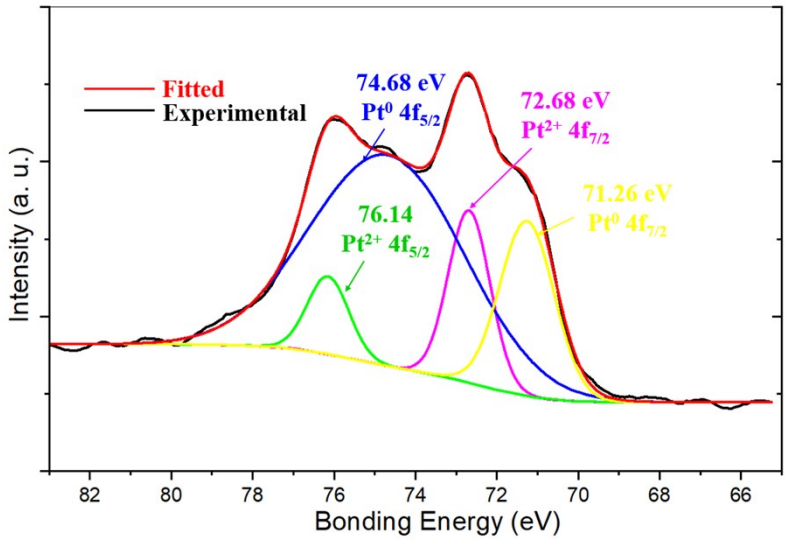

Figure S 77 The Pt 4f region in the XPS spectra of Pt@COF-DAI-TFP.

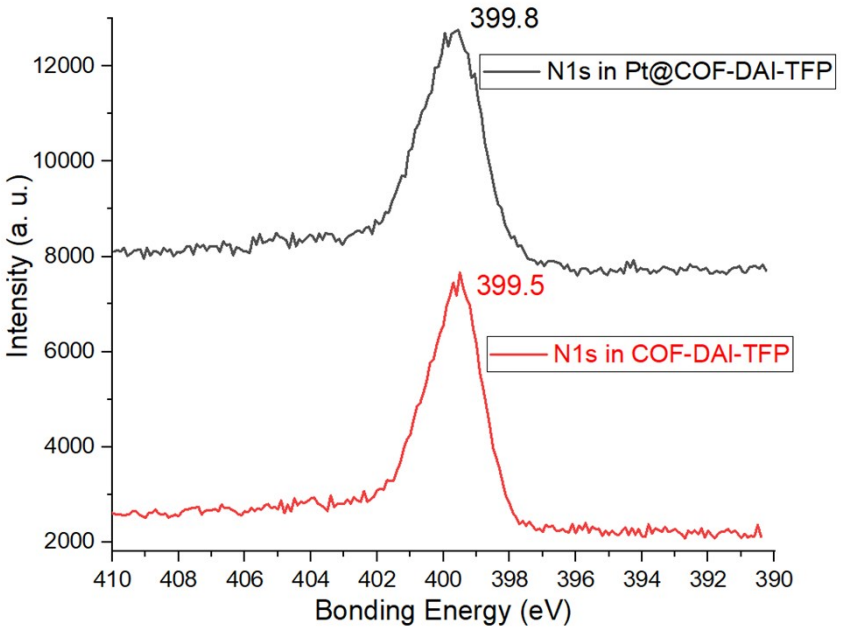

Figure S 78 The N 1S region in the XPS spectra of Pt@COF-DAI-TFP.

23. Summary of the typical performances of MNPs immobilized by various COFs.

Table S1 Summary of the typical performances of MNPs immobilized by various COFs.

Materials	Metal	Size (nm)	Metal Content (%)	Year	Ref.
COF-DAB-TFB	Pd	10	7.1	2011	[1]
COF-102	Pd	2.4± 0.5	30	2012	[2]
COF-DAB-TFP	Pd	10	6.4~ 10.2	2014	[3]
COF-DAB-TFP	Au	5	2.2	2014	[4]
COF-DETH-TFPT	Pt	10		2014	[5]
COF-Thio-TFP	Pd, Pt	Pd: 1.8, Pt: 1.7	Pd: 26.3, Pt: 34.3	2017	[6]
Phos-COF-1	Pd, Pt, Au	Pd: 1.62 Pt: 2.06 Au: 1.78	Pd: 2.84 Pt: 3.2 Au: 12.5	2020	[7]
This work	**Pd, Ir, Pt**	**Pd: 1.74, Ir: 1.99, Pt: 2.25**	**Pd: 20.47, Ir: 17.18, Pt: 29.46**	**2020**	**This Work**

1 Ding, S.; Gao, J.; Wang, Q.; Zhang, Y.; Song, W.; Su, C.; Wang, W. Construction of Covalent Organic Framework for Catalysis: Pd/COF-LZU1 in Suzuki-Miyaura Coupling Reaction. *J. Am. Chem. Soc.* **2011**, 133, 19816-19822.

2 Kalidindi, S. B.; Oh, H.; Hirscher, M.; Esken, D.; Wiktor, C.; Turner, S.; Tendeloo, G. V.; Fischer, R. A. Metal@COFs: Covalent Organic Frameworks as Templates for Pd Nanoparticles and Hydrogen Storage Properties of Pd@COF‐102 Hybrid Material. *Chem. Eur. J.* **2012**, 18, 10848-10856.

3 Díazbc, D. D.; Banerjee, R. Multifunctional and robust covalent organic framework-nanoparticle hybrids. *J. Mater. Chem. A* **2014**, 2, 7944-7952.

4 Pachfule, P.; Kandambeth, S.; Díazbc, D. D.; Banerjee, R. Highly stable covalent organic framework-Au nanoparticles hybrids for enhanced activity for nitrophenol reduction. *Chem. Commun.* **2014**, 50, 3169-3172.

5 Stegbauer, L.; Schwinghammer, K.; Lotsch, B. V. A hydrazone-based covalent organic framework for photocatalytic hydrogen production. *Chem. Sci.* **2014**, 5, 2789-2793.

6 Lu, S.; Hu, Y.; Wan, S.; McCaffrey, R.; Jin, Y.; Gu, H.; Zhang, W. Synthesis of Ultrafine and Highly Dispersed Metal Nanoparticles Confined in a Thioether-Containing Covalent Organic Framework and Their Catalytic Applications. *J. Am. Chem. Soc.* **2017**, 139, 17082-17088.

7 Tao, R.; Shen, X.; Hu, Y.; Kang, K.; Zheng, Y.; Luo, S.; Yang, S.; Li, W.; Lu, S.; Jin, Y.; Qiu, L.; Zhang, W. Phosphine-Based Covalent Organic Framework for the Controlled Synthesis of Broad-Scope Ultrafine Nanoparticles. *Small* **2020**, 16, 1906005.

24. M@COF-DAI-TFP catalyze the reduction of *p*-nitrophenol

General Procedure for the Reduction of 4-Nitrophenol Catalyzed by M@COF-DAI-TFP. To a cuvette was added an aqueous solution of 4-nitrophenol (1 mM, 0.3 mL), water (1 mL), and an aqueous solution of $NaBH_4$ (0.5 M, 1 mL). A suspension of M@COF-DAI-TFP in water (0.5 mg/mL, 35 μL) was introduced, and the reduction progress was monitored by the UV-vis spectroscopy. The initial bright yellow solution gradually turned to colorless.

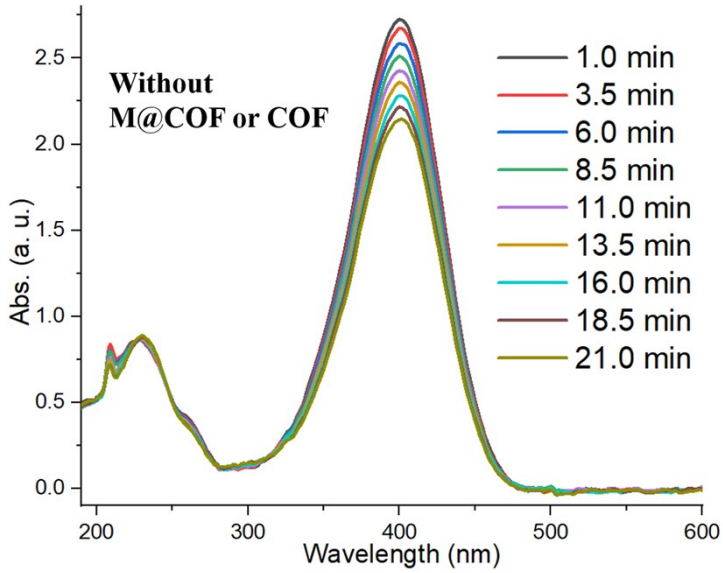

Figure S 79 Reduction of p-nitrophenol without COF-DAI-TFP or M@COF-DAI-TFP.

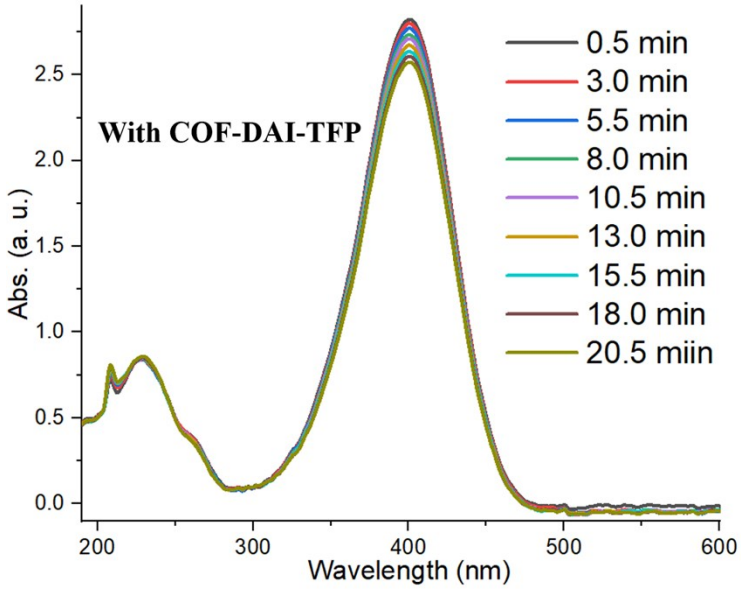

Figure S 80 Reduction of p-nitrophenol with COF-DAI-TFP.

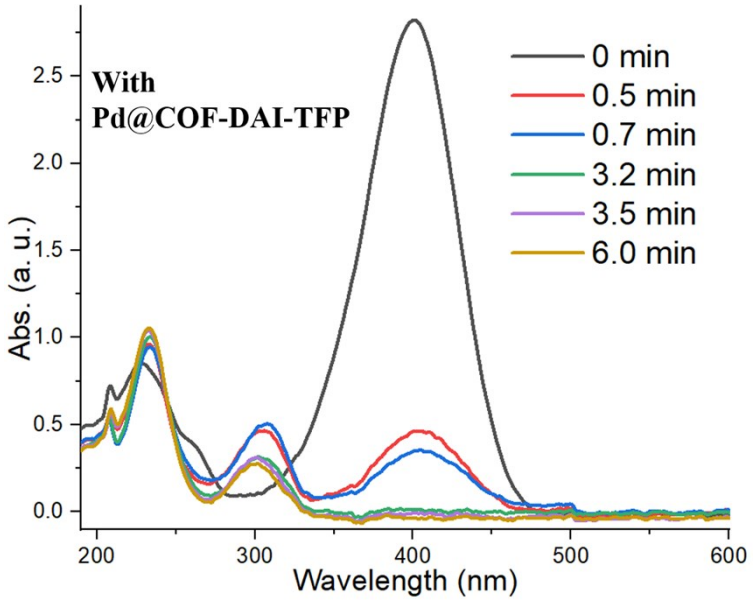

Figure S 81 Reduction of p-nitrophenol with Pd@COF-DAI-TFP.

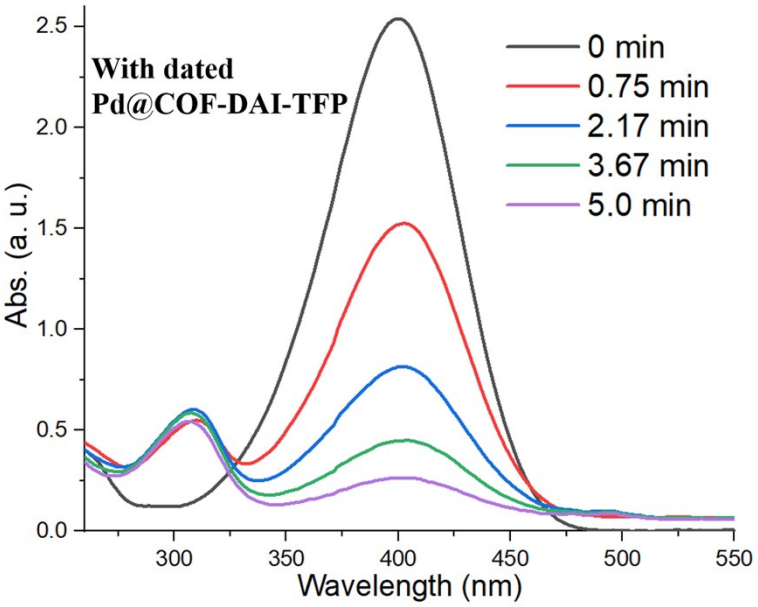

Figure S 82 Catalytic stability test of Pd@COF-DAI-TFP.

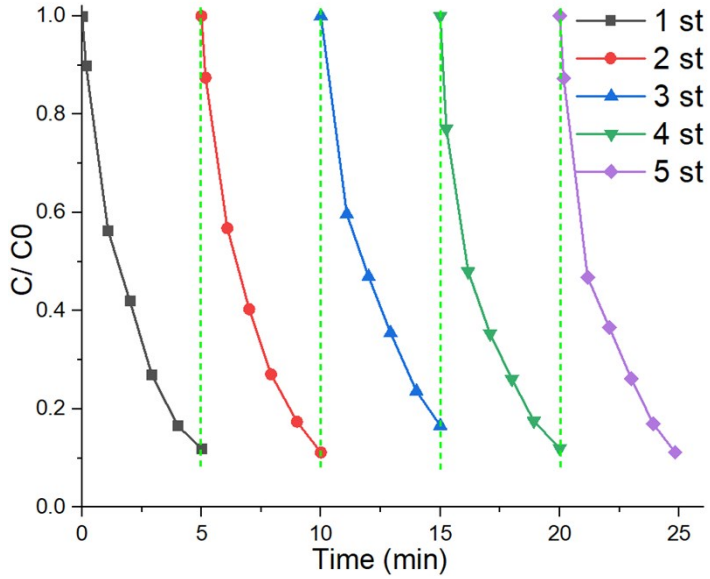

Figure S 83 Catalytic stability test of Pd@COF-DAI-TFP.

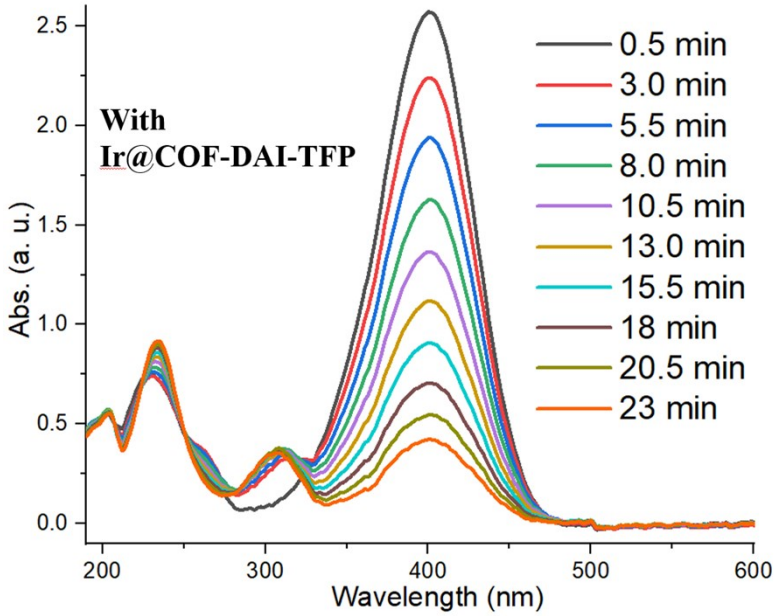

Figure S 84 Reduction of p-nitrophenol with Ir@COF-DAI-TFP.

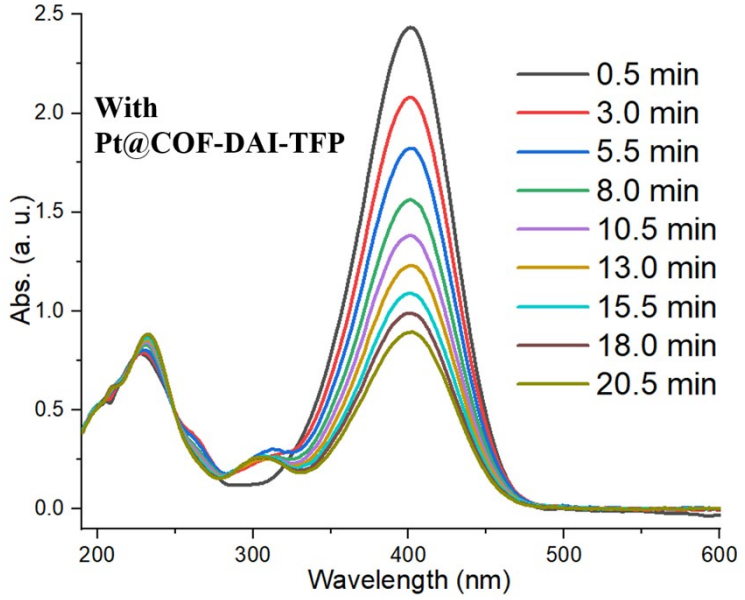

Figure S 85 Reduction of p-nitrophenol with Pt@COF-DAI-TFP.

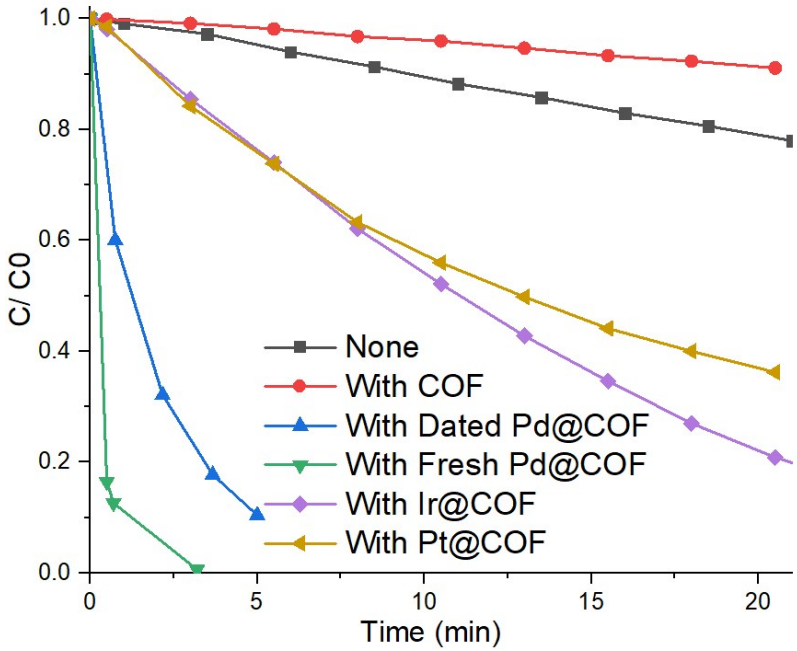

Figure S 86 Kinetic curve of p-nitrophenol reduction with different catalyst.